Geological Survey of Canada

CURRENT RESEARCH
2003-F3

SHRIMP U-Pb ages of granitoid basement rocks of the southwestern part of the Athabasca Basin, Saskatchewan and Alberta

R.A. Stern, C.D. Card, D. Pana, and N. Rayner

2003

Natural Resources Canada | Ressources naturelles Canada

Canada

CURRENT RESEARCH

©Her Majesty the Queen in Right of Canada 2003
ISSN 1701-4387

Available in Canada from the
Geological Survey of Canada Bookstore website at:
http://www.nrcan.gc.ca/gsc/bookstore (Toll-free: 1-888-252-4301)

A copy of this publication is also available for reference by depository libraries across Canada through access to the Depository Services Program's website at ***http://dsp-psd.pwgsc.gc.ca***

All requests for permission to reproduce this work, in whole or in part, for purposes of commercial use, resale, or redistribution shall be addressed to: Earth Sciences Sector Information Division, Room 402, 601 Booth Street, Ottawa, Ontario K1A 0E8.

Authors' addresses

R.A. Stern *(rstern@nrcan.gc.ca)*
N. Rayner *(nrayner@nrcan.gc.ca)*
J.C. Roddick (SHRIMP) Ion
Microprobe Labratory
Continental Geoscience Division
Geological Survey of Canada
Natural Resources Canada
601 Booth Street
Ottawa, Ontario K1A 0E8

C.D. Card *(ccard@ir.gov.sk.ca)*
Saskatchewan Industry and Resources
2101 Scarth Street
Regina, Saskatchewan S4P 3V7

D. Pana *(dpanagap@nrcan.gc.ca)*
Alberta Geological Survey
4th floor, Twin Atria
4999, 98th Avenue
Edmonton, Alberta T6B 2X3

Publication approved by Continental Geoscience Division

106-03634/

SHRIMP U-Pb ages of granitoid basement rocks of the southwestern part of the Athabasca Basin, Saskatchewan and Alberta

R.A. Stern, C.D. Card, D. Pana, and N. Rayner

Stern, R.A., Card, C.D., Pana, D., and Rayner, N., 2003: SHRIMP U-Pb ages of granitoid basement rocks of the southwestern part of the Athabasca Basin, Saskatchewan and Alberta; Radiogenic Age and Isotopic Studies: Report 16; Geological Survey of Canada, Current Research 2003-F3, 20 p.

Abstract: Zircons from seven granitoid samples from the southern and southwestern margins of the Athabasca Basin were dated using the SHRIMP II ion microprobe. A granite from the Virgin River shear zone was imprecisely dated at ca. 1.83 Ga. Two samples from the eastern Lloyd Domain both crystallized at ca. 1.98 Ga. These rocks were either sourced within, or intruded, 2.4–2.0 Ga crust. The Clearwater Domain comprises 1.843 Ga granite and 2.53 Ga granitic gneiss. Two granodioritic rocks within the basement at the western edge of the basin crystallized at 1.97 Ga. The new ages indicate that a considerable proportion of the basement to the western half of the Athabasca Basin is underlain by rocks related to the Taltson magmatic zone.

Résumé : Au moyen de la microsonde ionique SHRIMP II, on a daté des zircons provenant de sept échantillons de granitoïde prélevés le long des marges sud et sud-ouest du bassin d'Athabasca. Un granite de la zone de cisaillement de Virgin River a été daté de manière imprécise à environ 1,83 Ga. Deux échantillons prélevés dans la partie est du Domaine de Lloyd ont cristallisé à environ 1,98 Ga. Ces roches ont été formées ou mises en place par intrusion dans une partie de la croûte datant de 2,4-2,0 Ga. Le Domaine de Clearwater renferme du granite datant de 1,843 Ga et du gneiss granitique de 2,53 Ga. Le long de la marge ouest du bassin, deux roches granodioritiques du socle ont cristallisé à 1,97 Ga. Les résultats de ces nouvelles datations indiquent qu'une grande partie du socle sur lequel repose la moitié ouest du bassin d'Athabasca se compose de roches apparentées à la zone magmatique de Taltson.

INTRODUCTION

A primary goal of the 2000–2003 EXTECH IV Athabasca Uranium Multidisciplinary Study (Jefferson et al., 2002) was to enhance our knowledge of this uraniferous, ca. 1.7 Ga intracontinental sedimentary basin overlying diverse Archean and Paleoproterozoic basement rocks (Fig. 1). As a component of the subproject (#11) charged with addressing questions of the fourth ('time') dimension, a number of crystalline basement samples were targeted for U-Pb geochronology. The samples were obtained from the western half of the basin owing to the paucity of geochronological data from this region, in contrast to the relatively well constrained geochronological framework established at the southeastern

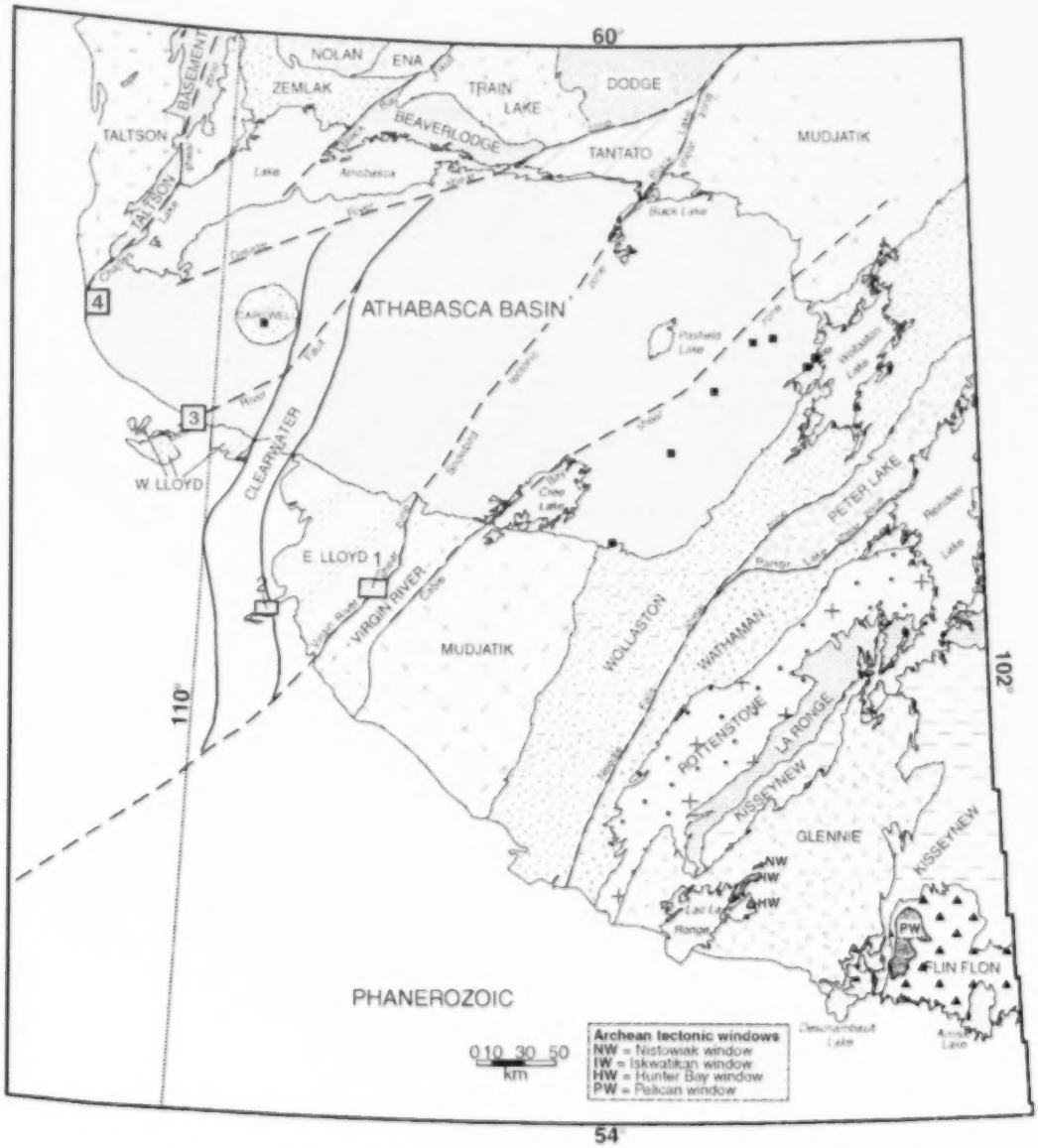

Figure 1. *Domainal map of the Precambrian Shield in northern Saskatchewan and northeastern Alberta showing the areas from which the U-Pb geochronology samples for this study were collected. Box marked '1' indicates the Careen Lake area (Virgin River shear zone and eastern Lloyd Domain), from which z7472, z7473, and z7474 were obtained; '2': location of z7471 and z7475 from the Clearwater River area; '3': location of z7477 from the western Lloyd Domain; '4': location of z7478 from the Taltson magmatic zone. Small filled boxes in the basin are locations of uranium mines.*

INTRODUCTION

A primary goal of the 2000–2003 EXTECH IV Athabasca Uranium Multidisciplinary Study (Jefferson et al., 2002) was to enhance our knowledge of this uraniferous, ca. 1.7 Ga intracontinental sedimentary basin overlying diverse Archean and Paleoproterozoic basement rocks (Fig. 1). As a component of the subproject (#11) charged with addressing questions of the fourth ('time') dimension, a number of crystalline basement samples were targeted for U-Pb geochronology. The samples were obtained from the western half of the basin owing to the paucity of geochronological data from this region, in contrast to the relatively well constrained geochronological framework established at the southeastern

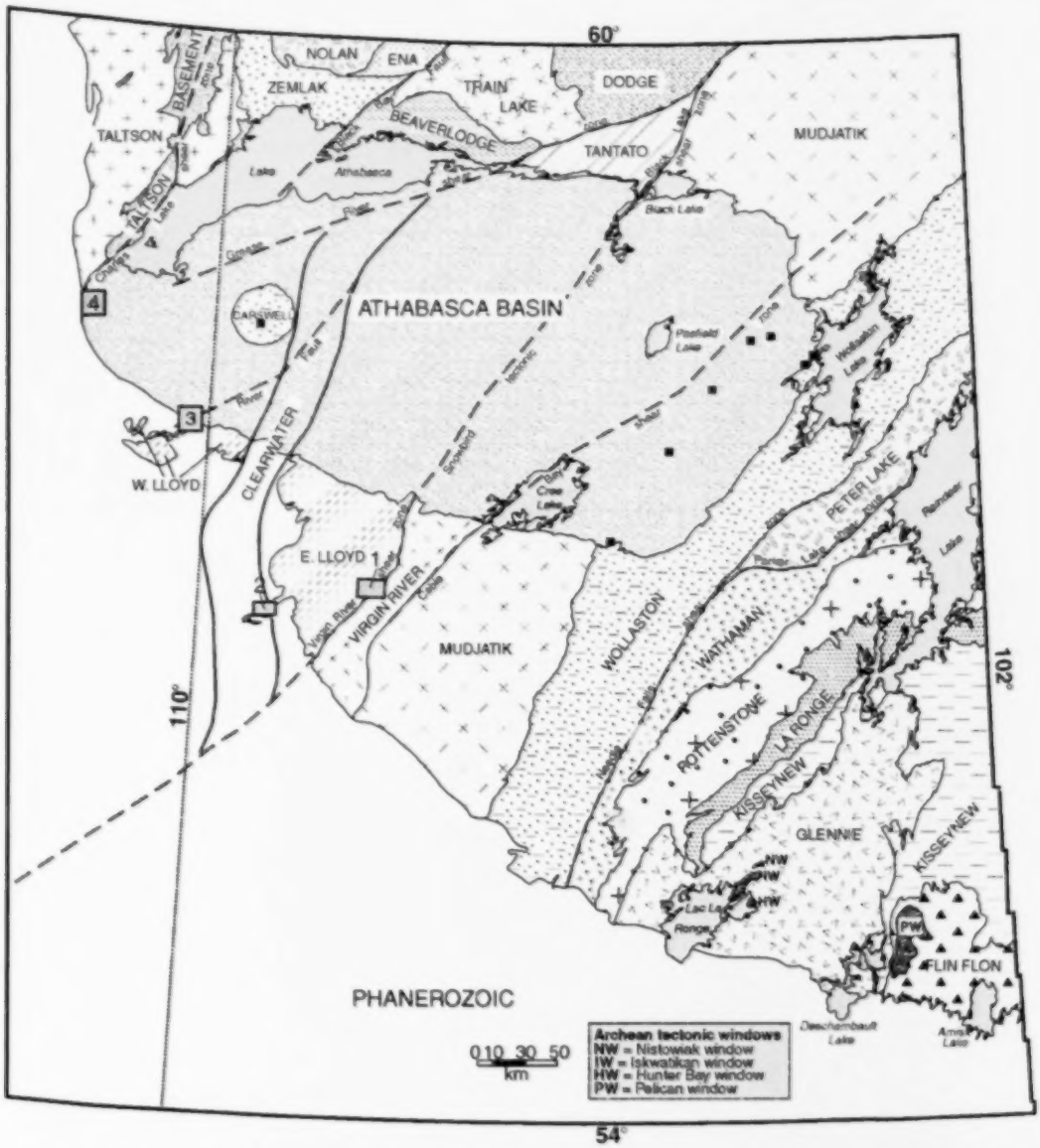

Figure 1. *Domainal map of the Precambrian Shield in northern Saskatchewan and northeastern Alberta showing the areas from which the U-Pb geochronology samples for this study were collected. Box marked '1' indicates the Careen Lake area (Virgin River shear zone and eastern Lloyed Domain), from which z7472, z7473, and z7474 were obtained; '2': location of z7471 and z7475 from the Clearwater River area; '3': location of z7477 from the western Lloyd Domain; '4': location of z7478 from the Taltson magmatic zone. Small filled boxes in the basin are locations of uranium mines.*

margin (e.g. Annesley et al., 1999). The interpretation of the subbasin geological framework is necessarily constrained largely by extrapolation of aeromagnetic patterns from exposed rocks lying beyond the basin margins, and a limited number of drill-core samples (Card, 2001). Both exposed basement samples and drill core are represented in this study, which utilized, for the first time within and around the basin, the SHRIMP ion microprobe (Stern, 1996) to determine U-Pb isotopic ages of zircons. The SHRIMP dating method is a well established method (e.g. Williams, 1998) with particularly strong attributes for recovering ages from the complex zircons often found in Precambrian metamorphic and igneous rocks.

SAMPLES

The seven rocks investigated here were obtained from major lithotectonic domains underlying the Athabasca Basin along its southwesterly and westerly margins (Card, 2001). Starting from the central Athabasca Basin, from east to west (Fig. 1) these are the Virgin River Domain, eastern Lloyd Domain (formerly Western Granulite domain), Clearwater Domain, western Lloyd Domain (formerly Firebag domain), and Taltson magmatic zone.

Virgin River Domain

At its western margin, the Virgin River Domain comprises a composite shear zone (the Virgin River shear zone; Fig. 1) containing dominantly high-grade felsic gneiss and a sliver of middle amphibolite-facies supracrustal rocks. Younger, less deformed mafic dykes and granitoid rocks intrude the gneiss. Shearing has involved a wide zone of east-vergent reverse motion and two narrower and younger zones recording dextral displacement. Sample z7474 (field # 0261-59) is a medium-grained, equigranular, biotite granite (Fig. 2a) obtained from the older of the two belts characterized by dextral shear (box '1' in Fig. 1). In contrast to the mylonitic rocks in this belt, this rock exhibits only a very weak northeast-trending fabric indicating that it experienced only the waning stages of deformation. The crystallization age should provide a minimum age for shearing in this belt, however, it is considered older than the last phase of dextral shearing in the

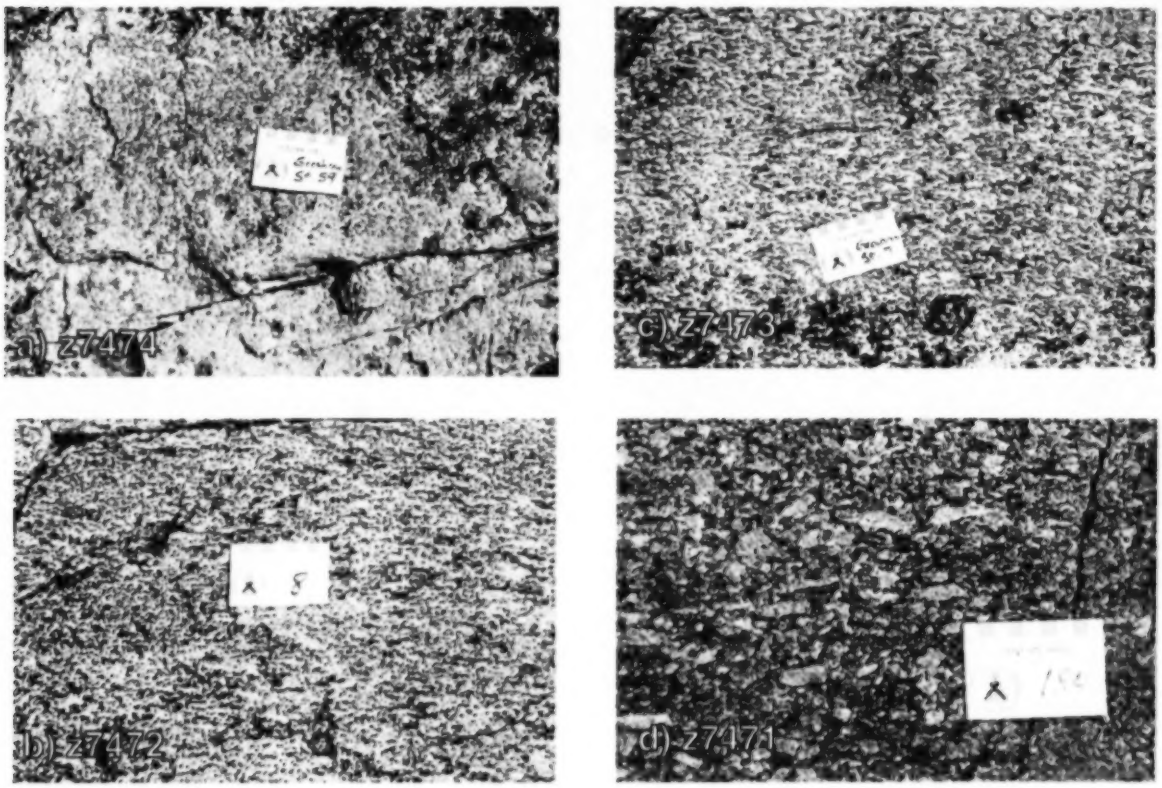

Figure 2. *Photographs of dated rock samples.* ***a)*** *z7474, aplitic granite, Virgin River shear zone;* ***b)*** *z7472, quartz diorite, eastern Lloyd Domain;* ***c)*** *z7473, leucogranite, eastern Lloyd Domain;* ***d)*** *z7471, granite, Clearwater Domain.*

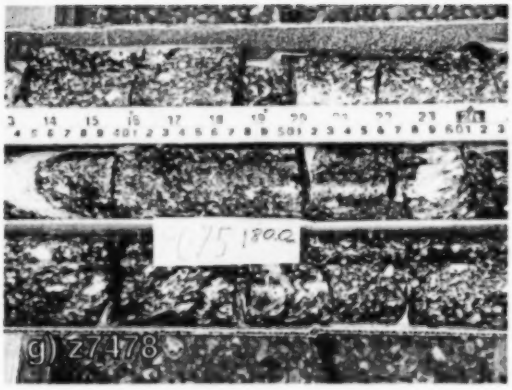

Figure 2. (cont.) ***e)*** *z7475, granitoid gneiss, Clearwater Domain;* ***f)*** *z7477, granodiorite, Maybelle River area;* ***g)*** *z7478, Fishing Creek quartz diorite.*

Virgin River shear zone. This sample is a possible equivalent of another unit previously dated within the domain, the 1820 Ma Junction Granite (Bickford et al., 1994).

Eastern Lloyd Domain

Both the eastern and western segments of the Lloyd Domain are similar in containing mainly granulite-facies rocks, comprising mainly an old supracrustal package that was intruded by ultramafic rocks and a polydeformed quartz diorite suite. Most rocks in the Lloyd Domain have been subjected to two phases of high-grade metamorphism: the first reaching granulite facies as indicated by orthopyroxene-bearing diatexite and the second at least upper amphibolite facies. The Careen Lake area of the eastern Lloyd Domain (box '1' in Fig. 1) is dominated by a suite of mainly quartz dioritic rocks that intrude the Careen Lake Group, a package of high-grade metasedimentary rocks. The quartz diorite suite generally comprises equigranular, magnetiferous gabbroic to quartz monzonitic rocks varying in colour index from 10 to 50. Quartz diorite is generally medium grained, and contains 25–40% hornblende plus biotite. Hornblende was likely dominant originally but has been largely replaced by aggregates of biotite and hornblende due to the cumulative affects of two high-grade metamorphic events. Magnetite is ubiquitous and the high magnetic susceptibility of these rocks is considered to be responsible for the magnetic highs of the Lloyd Domain. The quartz diorite suite was deformed during at least four ductile events.

Metre-scale bodies of medium-grained, pink granite containing 1–3% biotite, commonly associated with the quartz diorite suite, are found in the eastern Lloyd Domain. These granitic rocks were strongly deformed during the final three ductile deformation events but apparently lack first-phase structures, and were therefore interpreted to be younger than the quartz diorite, although no intrusive relationship was identified.

Two 30 kg samples were obtained from outcrop in the Careen Lake area (box '1' in Fig. 1). Sample z7472 (field # 0261-5) is a quartz diorite (Fig. 2b) from the shoreline exposure at Careen Lake, a representative of the magnetite-bearing quartz diorite suite which comprises the dominant lithology in the area. This sample should provide a minimum age for the Careen Lake Group and a maximum age for ductile deformation and high-grade metamorphism preserved in these rocks. The second sample, z7473 (field # 0261-7) was obtained from a leucogranite body (Fig. 2c) concordant with and containing a southwest-trending, strong foliation formed during F_2 folding. The sample should provide a maximum age for the southwest-trending folds in the area.

Clearwater Domain

The Clearwater Domain (Fig. 1) is a poorly exposed, granitoid terrain characterized by a prominent aeromagnetic high. The eastern portion of the domain is underlain by the late, multiphase Clearwater granite which contains large xenoliths of older granitic gneiss. The western part of the exposed Clearwater Domain is dominated by granitic gneiss (Sibbald, 1974) considered by Lewry and Sibbald (1977) to be more analogous to gneiss of the Mudjatik Domain than those of the eastern Lloyd Domain (Fig. 1). Sample z7471 (field #0261-184) was obtained from the porphyritic phase of the Clearwater granite suite (box '2' in Fig. 1). Approximately 20 kg of a weakly deformed, medium- to coarse-grained, K-feldspar-phyric biotite (5–10%) granite (Fig. 2d) were processed. It is interpreted as broadly comagmatic with equigranular granite which outcrops to the east of it. Potassium feldspar phenocrysts are up to 4 cm in long dimension and commonly help to define a tectonic foliation. The rock is texturally similar to the aforementioned Junction Granite.

A second large sample collected, z7475 (field #0261-186), is a foliated, medium-grained granitoid gneiss xenolith (Fig. 2e) found within the equigranular phase of the Clearwater granite. The sample is representative of the western gneissic rocks of the Clearwater Domain, and should provide age constraints on the rocks intruded by the younger Clearwater granite.

Western Lloyd Domain

A small sample from a mineral exploration drill core was collected from a northerly sub-Athabasca basement extension of the western Lloyd Domain. The sample, z7477 (field # 3502; drill hole FC 98-78.6m; box 3 in Fig. 1), is a sample of coarse-grained, virtually undeformed granodiorite (Fig. 2f). This 'Wylie-type' granodiorite (*see* below) is interpreted to comprise most of the Alberta part of the sub-Athabasca Basin basement.

Taltson magmatic zone

The southern portion of the Taltson magmatic zone is exposed immediately to the north of the Athabasca Basin (Fig. 1), and is characterized by basement gneiss, amphibolite, and meta-supracrustal rocks (3.3–3.0 Ga, 2.6 Ga, 2.4–2.1 Ga) intruded by voluminous, ca. 1.99–1.92 continental arc (I-type) and collisional (S-type) magmatic rocks (e.g. McDonough et al., 2000; McNicoll et al., 2000). Based on its aeromagnetic signature, the basement to the Athabasca Basin in Alberta has commonly been interpreted as a western extension of the southern Rae Province (e.g. Ross et al., 1991) and therefore potentially Archean. In contrast, Wilson (1986) suggested that most of those rocks were equivalents of the ca. 1963 Ma Wylie Lake granodiorite (McDonough et al., 2000) of the Taltson magmatic zone which is exposed immediately north of Lake Athabasca.

A mineral exploration drill core sample, z7478 (field # 3503, informally, the 'Fishing Creek' quartz diorite; drill hole FC 75-180m; box '4' in Fig. 1), was collected from the western edge of the Athabasca Basin (Fig. 1). It is a weakly deformed, medium-grained, grey, quartz diorite (Fig. 2g).

ANALYTICAL TECHNIQUES

The SHRIMP analytical procedures followed those described in detail elsewhere (Stern, 1997; Stern, 2001; Stern and Amelin, 2003). Briefly, zircons were cast in a 2.5 cm diameter epoxy mount (GSC #IP279) along with fragments of the GSC laboratory standard zircon (z6266, with $^{206}Pb/^{238}U$ age = 559 Ma). The mid-sections of the zircons were exposed using diamond compound, and the internal features of the zircons were characterized with backscattered electron(s) (BSE) utilizing a Cambridge Instruments scanning electron microscope. Mount surfaces were evaporatively coated with 10 nm of high purity Au. Analyses were conducted using an O^- primary beam, projected onto the zircons at 10 kV as elliptical spots of approximately 10 µm, 15 µm, or 30 µm in the longest dimension, and with uniform density beam currents of approximately 0.7 nA, 5 nA, and 20 nA, respectively. The count rates of ten isotopes of Zr^+, U^+, Th^+, and Pb^+ in zircon were sequentially measured (six scans) with a single electron multiplier and a pulse counting system with deadtime of 31 ns. Mass resolution was 5200 (1%) and ^{206}Pb sensitivity about 9 cps/ppm/nA in zircon. Off-line data processing was accomplished using customized in-house software.

The 1σ external errors of $^{206}Pb/^{238}U$ ratios reported in Table 1 incorporate a ±1.0% error in calibrating the standard zircon. No fractionation correction was applied to the Pb-isotope data; common Pb correction utilized the measured $^{204}Pb/^{206}Pb$ and compositions modelled after Cumming and Richards (1975). Decay constants are those of Jaffey et al. (1971). Mean square of weighted deviates (MSWD) and probability of equivalence (P) values were calculated using Isoplot v. 2.49 (Ludwig, 2001).

RESULTS

Raw analytical data are presented in Table 1, and a summary of age results in Table 2. Errors quoted in the text and error ellipses in the figures are at 2σ.

z7474 (aplitic granite, Virgin River shear zone)

In transmitted light and BSE images (Fig. 3) the zircons recovered comprise two main morphological types.

A) Prismatic grains (75–150 µm wide, aspect ratios of 1.5–2.5:1), ranging from clear, colourless to orange stained are the first type. In transmitted light, thin rims are visible in many, giving such grains relatively sharp edges. Backscattered electron images reveal a range of unzoned

Table 1. SHRIMP U-Pb zircon data for granitoid basement samples beneath the south and southwestern portions of the Athabasca Basin.

Spot name	Zircon generation (see text)	Spot size	U (ppm)	Th (ppm)	Th/U	Pb* (ppm)	^{204}Pb (ppb)	^{204}Pb/^{206}Pb	± ^{204}Pb/^{206}Pb	f(206)^{204}	^{208}Pb/^{232}Pb	± ^{208}Pb/^{232}Pb	^{207}Pb/^{235}U	± ^{207}Pb/^{235}U	^{206}Pb/^{238}U	± ^{206}Pb/^{238}U	Corr Coeff	^{207}Pb/^{206}Pb	± ^{207}Pb/^{206}Pb	Apparent ages (Ma) ^{206}Pb/^{238}U	±	^{206}Pb/^{238}U	^{207}Pb/^{206}Pb	± ^{207}Pb/^{206}Pb	Disc. (%)
z7474, aplitic granite, Virgin River shear zone																									
7474-26.1	2	10 µm	918	25	0.028	276	6	2.40E-05	1.54E-05	0.0004	0.0090	0.0009	4.679	0.104	0.3126	0.0063	0.951	0.10855	0.00075	1754	31	1775	13	1.2
7474-59.1	2	10 µm	1194	36	0.031	363	15	4.63E-05	2.30E-05	0.0008	0.0090	0.0011	4.811	0.119	0.3159	0.0067	0.910	0.11045	0.00114	1770	33	1807	19	2.1
7474-42.1	2	10 µm	1252	39	0.032	381	11	3.19E-05	1.71E-05	0.0006	0.0102	0.0013	4.837	0.103	0.3160	0.0062	0.959	0.11101	0.00068	1770	31	1816	11	2.5
7474-28.1	2	10 µm	1819	44	0.025	573	5	9.29E-06	1.41E-05	0.0002	0.0078	0.0008	5.053	0.106	0.3273	0.0064	0.968	0.11197	0.00059	1825	31	1832	10	0.4
7474-50.3	2	10 µm	665	114	0.178	243	19	9.03E-05	3.97E-05	0.0016	0.0455	0.0021	5.893	0.167	0.3649	0.0082	0.859	0.11714	0.00171	2005	39	1913	26	-4.8
7474-50.4	2	10 µm	740	44	0.062	257	10	4.52E-05	3.72E-05	0.0008	0.0218	0.0018	5.887	0.162	0.3529	0.0080	0.883	0.12098	0.00157	1948	38	1971	23	1.1
7474-50.2	2	10 µm	813	69	0.088	270	16	6.97E-05	3.60E-05	0.0012	0.0238	0.0018	5.885	0.266	0.3359	0.0069	0.562	0.12705	0.00479	1867	34	2058	68	9.3
7474-9.1	1	30 µm	37	1	0.018	11	1	1.47E-04	1.76E-04	0.0026	0.0037	0.0068	4.821	0.153	0.3172	0.0045	0.556	0.11025	0.00293	1776	22	1804	49	1.5
7474-9.2	1	30 µm	42	1	0.016	13	1	7.36E-05	6.10E-05	0.0013	0.0044	0.0023	5.093	0.063	0.3307	0.0038	0.782	0.11168	0.00114	1842	18	1827	19	-0.8
7474-9.3	1	30 µm	61	1	0.014	19	1	5.26E-05	3.28E-05	0.0009	0.0049	0.0013	5.112	0.079	0.3302	0.0041	0.866	0.11230	0.00088	1839	20	1837	14	-0.1
7474-51.1	1	30 µm	41	28	0.703	16	1	7.91E-05	4.34E-05	0.0014	0.2014	0.0033	5.380	0.076	0.3330	0.0036	0.838	0.11715	0.00091	1853	18	1913	14	3.1
7474-17.1	1	30 µm	59	122	2.129	30	0	1.11E-05	4.55E-05	0.0002	0.6056	0.0070	5.489	0.092	0.3372	0.0039	0.772	0.11806	0.00126	1873	19	1927	19	2.8
7474-49.1	1	30 µm	123	100	0.836	51	1	3.79E-05	1.21E-05	0.0007	0.2394	0.0027	5.814	0.070	0.3519	0.0038	0.930	0.11981	0.00054	1944	18	1953	8	0.5
7474-44.1	1	30 µm	117	72	0.635	45	1	1.58E-05	1.79E-05	0.0003	0.1803	0.0017	5.771	0.078	0.3474	0.0038	0.866	0.12048	0.00082	1922	18	1963	12	2.1
7474-68.1	1	30 µm	144	158	1.131	64	2	5.44E-05	1.57E-05	0.0009	0.3215	0.0033	5.986	0.285	0.3587	0.0091	0.632	0.12104	0.00451	1976	43	1972	68	-0.2
7474-67.1	1	30 µm	674	182	0.327	242	28	1.44E-04	2.62E-05	0.0025	0.0991	0.0022	8.026	0.402	0.3931	0.0049	0.365	0.14810	0.00895	2137	23	2324	83	8.1
z7472, quartz diorite, Lloyd Domain																									
7472-46.1	4	30 µm	33	4	0.136	11	0	1.77E-05	6.11E-05	0.0003	0.0404	0.0028	5.295	0.087	0.3347	0.0039	0.784	0.11475	0.00118	1861	19	1876	19	0.8
7472-12.1	4	30 µm	61	14	0.247	21	0	1.00E-05	1.00E-05	0.0002	0.0745	0.0011	5.367	0.065	0.3358	0.0037	0.947	0.11591	0.00046	1867	18	1894	7	1.5
7472-92.1	4	30 µm	50	10	0.205	17	0	3.36E-05	2.65E-05	0.0006	0.0598	0.0014	5.401	0.075	0.3377	0.0038	0.871	0.11601	0.00079	1876	18	1896	12	1.1
7472-29.1	4	30 µm	46	6	0.125	15	0	1.00E-05	1.00E-05	0.0002	0.0361	0.0009	5.421	0.079	0.3378	0.0040	0.870	0.11639	0.00085	1876	19	1902	13	1.3
7472-74.1	4	30 µm	106	20	0.200	36	1	3.58E-05	1.33E-05	0.0006	0.0564	0.0009	5.427	0.062	0.3381	0.0035	0.950	0.11644	0.00042	1877	17	1902	6	1.3
7472-105.2	3	30 µm	29	13	0.458	11	3	3.39E-04	8.29E-05	0.0059	0.1219	0.0042	5.246	0.109	0.3421	0.0047	0.743	0.11124	0.00155	1897	22	1820	26	-4.2
7472-101.2	3	30 µm	16	6	0.389	5	2	3.49E-04	2.19E-04	0.0060	0.1189	0.0090	5.091	0.196	0.3207	0.0059	0.582	0.11512	0.00362	1793	29	1882	58	4.7
7472-33.1	3	30 µm	11	1	0.137	4	1	4.81E-04	1.48E-04	0.0083	0.0363	0.0080	5.399	0.153	0.3324	0.0046	0.592	0.11759	0.00271	1850	22	1920	42	3.6
7472-30.1	3	30 µm	32	5	0.173	11	0	1.00E-05	1.00E-05	0.0002	0.0503	0.0021	5.640	0.072	0.3457	0.0038	0.907	0.11834	0.00064	1914	18	1931	10	0.9
7472-105.1	3	30 µm	29	13	0.468	11	1	1.34E-04	7.07E-05	0.0023	0.1277	0.0034	5.676	0.095	0.3437	0.0038	0.738	0.11978	0.00136	1904	18	1953	20	2.5
7472-101.1	3	30 µm	20	8	0.408	7	0	1.00E-05	1.00E-05	0.0002	0.1169	0.0028	5.754	0.086	0.3458	0.0039	0.829	0.12070	0.00102	1914	19	1967	15	2.7
7472-3.1	2	15 µm	1089	361	0.362	393	31	9.58E-05	1.01E-05	0.0017	0.1030	0.0010	5.552	0.072	0.3434	0.0040	0.939	0.11726	0.00053	1903	19	1915	8	0.6
7472-50.2	2	15 µm	944	459	0.502	357	3	1.00E-05	1.00E-05	0.0002	0.1443	0.0011	5.641	0.065	0.3488	0.0038	0.968	0.11731	0.00034	1929	18	1916	5	-0.7
7472-61.2	2	15 µm	344	52	0.155	114	1	1.38E-05	1.08E-05	0.0002	0.0429	0.0010	5.430	0.091	0.3330	0.0051	0.951	0.11824	0.00062	1853	25	1930	9	4
7472-71.1	2	15 µm	748	282	0.390	289	0	1.50E-07	5.38E-06	0.0000	0.1121	0.0016	5.950	0.104	0.3645	0.0053	0.888	0.11841	0.00095	2003	25	1932	15	-3.7
7472-85.1	2	15 µm	712	273	0.396	269	1	4.25E-06	5.37E-06	0.0001	0.1110	0.0029	5.837	0.195	0.3570	0.0082	0.768	0.11860	0.00256	1968	39	1935	39	-1.7
7472-82.1	2	15 µm	819	834	1.051	348	3	1.09E-05	5.78E-06	0.0002	0.3040	0.0016	5.685	0.063	0.3461	0.0036	0.956	0.11914	0.00039	1916	17	1943	6	1.4
7472-58.1	2	15 µm	924	438	0.489	349	3	1.00E-05	1.00E-05	0.0002	0.1414	0.0025	5.736	0.123	0.3486	0.0057	0.836	0.11935	0.00142	1928	28	1947	21	1
7472-100.2	2	15 µm	500	325	0.672	197	0	1.51E-06	7.26E-06	0.0000	0.1919	0.0029	5.730	0.075	0.3481	0.0041	0.937	0.11938	0.00055	1926	20	1947	8	1.1
7472-10.1	2	15 µm	575	277	0.499	220	2	1.00E-05	1.00E-05	0.0002	0.1414	0.0012	5.802	0.068	0.3520	0.0037	0.933	0.11953	0.00051	1944	18	1949	8	0.3
7472-69.1	2	15 µm	610	163	0.234	296	2	1.00E-05	1.00E-05	0.0002	0.0678	0.0009	5.900	0.081	0.3574	0.0044	0.937	0.11972	0.00058	1970	21	1952	9	-0.9
7472-38.1	2	15 µm	197	37	0.194	68	1	2.61E-05	2.00E-05	0.0005	0.0673	0.0015	5.595	0.088	0.3387	0.0046	0.922	0.11982	0.00073	1880	22	1954	11	3.8
7472-103.1	2	15 µm	587	276	0.487	220	2	1.00E-05	1.00E-05	0.0002	0.1388	0.0012	5.758	0.071	0.3468	0.0039	0.954	0.12041	0.00045	1919	19	1962	7	2.2
7472-44.1	2	15 µm	1625	845	0.537	648	1	1.42E-06	2.79E-06	0.0000	0.1540	0.0009	6.047	0.073	0.3621	0.0040	0.950	0.12114	0.00046	1992	19	1973	7	-1
7472-89.1	2	15 µm	1888	841	0.460	734	6	1.00E-05	1.00E-05	0.0002	0.1301	0.0009	6.072	0.081	0.3611	0.0044	0.948	0.12194	0.00052	1988	21	1985	8	-0.1
7472-61.1	2	15 µm	326	184	0.584	130	1	1.00E-05	1.00E-05	0.0002	0.1694	0.0023	6.052	0.072	0.3597	0.0038	0.923	0.12204	0.00057	1981	18	1986	8	0.3
7472-93.1	2	15 µm	219	122	0.575	85	2	3.03E-05	2.39E-05	0.0005	0.1641	0.0027	5.933	0.124	0.3524	0.0047	0.721	0.12211	0.00179	1946	22	1987	26	2.1
7472-44.2	2	15 µm	929	603	0.671	398	12	4.06E-05	8.47E-06	0.0007	0.1962	0.0012	6.384	0.075	0.3777	0.0041	0.958	0.12258	0.00042	2066	19	1994	6	-3.6
7472-89.2	2	15 µm	741	444	0.620	292	2	1.11E-05	6.60E-06	0.0002	0.1783	0.0019	6.008	0.074	0.3519	0.0039	0.940	0.12381	0.00052	1944	19	2012	8	3.4
7472-32.1	1	15 µm	193	74	0.395	76	2	2.49E-05	2.54E-05	0.0004	0.1111	0.0019	6.623	0.092	0.3667	0.0041	0.865	0.13028	0.00092	2023	19	2102	12	3.7
7472-76.1	1	15 µm	235	142	0.624	104	5	6.21E-05	2.35E-05	0.0011	0.1754	0.0044	7.709	0.172	0.3894	0.0065	0.820	0.14356	0.00184	2120	30	2271	22	6.6
7472-14.1	1	15 µm	253	102	0.417	116	0	2.81E-06	1.57E-05	0.0001	0.1234	0.0018	8.780	0.115	0.4190	0.0045	0.873	0.15198	0.00098	2256	20	2368	11	4.7
7472-77.2	1	15 µm	361	155	0.459	179	2	1.44E-05	1.08E-05	0.0003	0.1280	0.0021	9.949	0.119	0.4628	0.0050	0.948	0.15593	0.00080	2452	22	2412	7	-1.7
z7473, leucogranite, Lloyd Domain																									
7473-45.2	3	15 µm	393	192	0.506	149	1	5.00E-06	9.00E-06	0.0001	0.1416	0.0016	5.708	0.093	0.3507	0.0043	0.826	0.11805	0.00109	1938	21	1927	17	-0.6
7473-20.2	2	30 µm	1147	143	0.129	403	1	1.66E-06	1.49E-06	0.0000	0.0348	0.0002	5.699	0.075	0.3553	0.0044	0.969	0.11635	0.00038	1960	21	1901	6	-3.1
7473-6.1	2	30 µm	267	115	0.446	98	2	2.60E-05	9.93E-06	0.0005	0.1244	0.0010	5.501	0.084	0.3427	0.0041	0.844	0.11640	0.00096	1900	20	1902	15	0.1
7473-35.1	2	15 µm	277	132	0.492	99	1	8.84E-06	1.63E-05	0.0002	0.1400	0.0019	5.312	0.075	0.3294	0.0041	0.917	0.11696	0.00067	1835	20	1910	10	3.9
7473-46.2	2	15 µm	6249	967	0.160	2160	3	1.47E-06	5.70E-07	0.0000	0.0459	0.0002	5.855	0.078	0.3487	0.0047	0.991	0.11760	0.00022	1928	23	1920	3	-0.4
7473-105.1	2	15 µm	504	95	0.196	173	1	7.89E-06	9.07E-06	0.0001	0.0567	0.0014	5.535	0.072	0.3404	0.0040	0.934	0.11793	0.00055	1889	19	1925	8	1.9
7473-48.1	2	30 µm	382	269	0.726	148	1	9.37E-06	8.70E-06	0.0002	0.2065	0.0011	5.454	0.073	0.3349	0.0037	0.887	0.11810	0.00074	1862	18	1928	11	3.4
7473-46.1	2	15 µm	859	206	0.248	300	3	1.27E-05	5.94E-06	0.0002	0.0722	0.0008	5.576	0.076	0.3410	0.0040	0.913	0.11861	0.00066	1891	19	1935	10	2.3
7473-22.1	2	30 µm	247	103	0.433	90	1	1.58E-05	9.33E-06	0.0003	0.1261	0.0018	5.596	0.146	0.3421	0.0044	0.593	0.11863	0.00251	1897	21	1936	38	2
7473-60.1	2	30 µm	191	136	0.737	75	2	3.38E-05	9.68E-06	0.0008	0.2101	0.0016	5.614	0.088	0.3425	0.0043	0.866	0.11868	0.00094	1899	21	1939	14	2.1
7473-64.1	2	30 µm	255	118	0.478	92	2	2.68E-05	8.16E-06	0.0005	0.1374	0.0011	5.516	0.091	0.3353	0.0052	0.967	0.11930	0.00051	1864	25	1946	8	4.2
7473-42.1	2	30 µm	1217	163	0.139	432	4	1.00E-05	1.00E-05	0.0002	0.0416	0.0006	5.850	0.080	0.3556	0.0045	0.956	0.11931	0.00048	1961	21	1946	7	-0.8
7473-91.1	2	30 µm	241	97	0.417	88	1	7.75E-06	8.40E-06	0.0001	0.1200	0.0009	5.631	0.074	0.3419	0.0041	0.947	0.11945	0.00051	1896	20	1948	8	2.7
7473-62.1	2	30 µm	303	107	0.363	109	6	7.24E-05	1.12E-05	0.0013	0.1029	0.0009	5.623	0.078	0.3414	0.0040	0.904	0.11945	0.00071	1893	19	1948	11	2.8

Table 1. (cont.)

Spot name	Zircon generation (see text)	Spot size	U (ppm)	Th (ppm)	Th/U	Pb* (ppm)	^{204}Pb (ppb)	^{204}Pb/^{206}Pb	± ^{204}Pb/^{206}Pb	f(206)^{204}	^{208*}Pb/^{206*}Pb	± ^{208}Pb/^{206}Pb	^{207*}Pb/^{235}U	± ^{207}Pb/^{235}U	^{206*}Pb/^{238}U	± ^{206}Pb/^{238}U	Corr Coeff	^{207*}Pb/^{206*}Pb	± ^{207}Pb/^{206}Pb	Apparent ages (Ma) ^{206}Pb/^{238}U	±	^{207}Pb/^{206}Pb	±	Disc. (%)
7473-11.1	2	30 µm	371	172	0.478	137	1	5.38E-06	6.26E-06	0.0001	0.1378	0.0008	5.627	0.089	0.3412	0.0042	0.837	0.11963	0.00105	1892	20	1951	16	3
7473-34.1	2	30 µm	205	111	0.559	77	1	1.00E-05	1.00E-05	0.0002	0.1619	0.0016	5.583	0.090	0.3379	0.0038	0.779	0.11981	0.00123	1877	19	1953	18	3.9
7473-83.1	2	30 µm	794	197	0.256	287	2	1.00E-05	1.00E-05	0.0002	0.0716	0.0006	5.862	0.080	0.3528	0.0043	0.943	0.12051	0.00055	1948	21	1964	8	0.8
7473-21.1	2	30 µm	753	168	0.230	269	2	7.43E-06	2.57E-06	0.0001	0.0655	0.0008	5.816	0.077	0.3499	0.0040	0.909	0.12053	0.00067	1934	19	1964	10	1.5
7473-77.1	2	30 µm	258	129	0.518	103	2	2.16E-05	7.48E-06	0.0004	0.1471	0.0019	6.113	0.145	0.3678	0.0067	0.831	0.12057	0.00161	2019	31	1965	24	-2.8
7473-70.1	2	15 µm	781	186	0.246	278	2	8.15E-06	5.15E-06	0.0001	0.0695	0.0008	5.772	0.077	0.3472	0.0042	0.953	0.12058	0.00049	1921	20	1965	7	2.2
7473-68.1	2	30 µm	740	179	0.250	270	3	1.38E-05	4.38E-06	0.0002	0.0705	0.0007	5.922	0.089	0.3560	0.0046	0.914	0.12067	0.00074	1963	22	1966	11	0.2
7473-106.2	2	30 µm	1261	148	0.122	448	3	8.25E-06	2.72E-06	0.0001	0.0357	0.0003	5.944	0.072	0.3572	0.0039	0.941	0.12070	0.00050	1969	18	1967	7	-0.1
7473-107.1	2	30 µm	796	227	0.294	289	1	5.74E-06	3.20E-06	0.0001	0.0853	0.0006	5.827	0.078	0.3494	0.0042	0.947	0.12097	0.00052	1932	20	1971	8	2
7473-40.1	2	30 µm	903	244	0.279	330	3	1.00E-05	1.00E-05	0.0002	0.0800	0.0005	5.899	0.077	0.3536	0.0040	0.923	0.12098	0.00061	1952	19	1971	9	1
7473-20.1	2	30 µm	742	196	0.272	271	45	2.01E-04	1.04E-05	0.0035	0.0840	0.0006	5.884	0.088	0.3525	0.0049	0.969	0.12107	0.00045	1947	24	1972	7	1.3
7473-64.1	2	30 µm	933	244	0.270	328	1	5.37E-06	2.16E-06	0.0001	0.0774	0.0004	5.696	0.071	0.3409	0.0037	0.919	0.12119	0.00060	1891	18	1974	9	4.2
7473-63.2	2	30 µm	899	252	0.290	329	1	4.30E-06	3.10E-06	0.0001	0.0830	0.0005	5.911	0.089	0.3536	0.0049	0.963	0.12125	0.00050	1952	24	1975	7	1.2
7473-102.1	2	30 µm	288	98	0.351	104	1	1.63E-05	6.13E-06	0.0003	0.1039	0.0008	5.738	0.077	0.3429	0.0041	0.945	0.12135	0.00054	1901	20	1976	8	3.8
7473-84.1	2	30 µm	271	114	0.435	102	0	3.42E-06	1.36E-05	0.0001	0.1276	0.0012	5.863	0.090	0.3503	0.0040	0.825	0.12138	0.00106	1936	19	1977	16	2
7473-50.1	2	30 µm	282	134	0.491	106	1	8.05E-06	7.37E-06	0.0001	0.1404	0.0010	5.805	0.086	0.3460	0.0047	0.953	0.12167	0.00055	1915	23	1981	8	3.3
7473-63.1	2	30 µm	884	248	0.289	317	2	8.93E-06	3.75E-06	0.0002	0.0836	0.0007	5.806	0.082	0.3459	0.0044	0.943	0.12173	0.00058	1915	21	1982	8	3.4
7473-106.1	2	30 µm	1095	141	0.133	379	2	5.14E-06	1.93E-06	0.0001	0.0378	0.0003	5.822	0.094	0.3467	0.0048	0.913	0.12178	0.00081	1919	23	1982	12	3.2
7473-45.1	2	15 µm	701	147	0.217	245	1	6.19E-06	6.49E-06	0.0001	0.0609	0.0007	5.792	0.081	0.3429	0.0044	0.951	0.12252	0.00054	1900	21	1993	8	4.7
7473-40.2	2	30 µm	747	225	0.311	268	1	5.50E-06	2.73E-06	0.0001	0.0890	0.0005	5.816	0.081	0.3435	0.0044	0.952	0.12279	0.00053	1904	21	1997	8	4.7
7473-15.1	1	15 µm	261	194	0.766	103	2	2.81E-05	1.71E-05	0.0005	0.2267	0.0028	5.877	0.086	0.3371	0.0042	0.908	0.12646	0.00078	1872	20	2049	11	8.6
z7471, granite, Clearwater Domain																								
7471-45.1	3	15 µm	930	34	0.038	290	6	2.38E-05	7.41E-06	0.0004	0.0117	0.0004	4.956	0.056	0.3227	0.0034	0.955	0.11138	0.00038	1803	16	1822	6	1
7471-60.2	2	15 µm	616	223	0.374	215	45	2.57E-04	4.44E-05	0.0045	0.1141	0.0031	5.096	0.077	0.3305	0.0037	0.804	0.11182	0.00102	1841	18	1829	17	-0.6
7471-15.1	2	15 µm	452	68	0.155	148	1	1.00E-05	1.00E-05	0.0002	0.0432	0.0008	5.076	0.070	0.3290	0.0036	0.852	0.11190	0.00081	1833	17	1831	13	-0.2
7471-57.2	2	15 µm	2500	688	0.284	816	1	1.86E-06	2.31E-06	0.0000	0.0818	0.0006	4.919	0.054	0.3178	0.0033	0.976	0.11225	0.00027	1779	16	1836	4	3.1
7471-76.1	2	15 µm	753	1705	2.341	381	5	2.32E-05	6.88E-06	0.0004	0.6812	0.0026	5.079	0.059	0.3273	0.0035	0.951	0.11257	0.00041	1825	17	1841	7	0.9
7471-60.1	2	15 µm	580	140	0.250	194	5	3.31E-05	9.98E-06	0.0006	0.0724	0.0009	5.097	0.063	0.3282	0.0036	0.931	0.11263	0.00051	1830	17	1842	8	0.7
7471-68.1	2	15 µm	781	224	0.297	270	2	1.01E-05	6.35E-06	0.0002	0.0888	0.0014	5.186	0.065	0.3339	0.0038	0.942	0.11266	0.00047	1857	18	1843	8	-0.8
7471-38.1	2	15 µm	511	179	0.362	172	8	5.84E-05	1.42E-05	0.0010	0.1022	0.0012	5.019	0.064	0.3231	0.0036	0.934	0.11268	0.00052	1805	18	1843	8	2.1
7471-57.1	2	15 µm	1934	507	0.271	658	1	2.31E-06	2.86E-06	0.0000	0.0782	0.0005	5.162	0.055	0.3319	0.0034	0.981	0.11281	0.00024	1847	16	1845	4	-0.1
7471-76.2	2	15 µm	803	224	0.385	211	0	2.18E-06	7.48E-06	0.0000	0.1121	0.0024	5.170	0.080	0.3321	0.0047	0.952	0.11291	0.00054	1849	23	1847	9	-0.1
7471-28.1	2	15 µm	1540	1037	0.696	581	2	5.09E-06	4.36E-06	0.0001	0.2003	0.0008	5.200	0.060	0.3338	0.0037	0.980	0.11297	0.00026	1857	18	1848	4	-0.5
7471-26.2	2	15 µm	533	743	1.441	232	11	7.13E-05	1.22E-05	0.0012	0.4159	0.0030	5.159	0.075	0.3307	0.0041	0.899	0.11316	0.00073	1842	20	1851	12	0.5
7471-51.1	1	30 µm	48	38	0.809	19	1	8.88E-05	3.72E-05	0.0015	0.2268	0.0025	5.228	0.070	0.3353	0.0036	0.857	0.11311	0.00079	1864	17	1850	13	-0.7
7471-96.2	1	30 µm	46	90	2.012	21	1	5.99E-05	7.09E-05	0.0010	0.5680	0.0077	4.865	0.166	0.3096	0.0067	0.724	0.11396	0.00271	1739	33	1864	44	6.7
7471-80.1	1	30 µm	167	96	0.594	62	1	2.52E-05	9.47E-06	0.0004	0.1734	0.0011	5.259	0.061	0.3345	0.0035	0.942	0.11402	0.00045	1860	17	1865	7	0.2
7471-80.2	1	30 µm	115	93	0.840	44	3	8.24E-05	2.21E-05	0.0014	0.2443	0.0023	5.148	0.089	0.3267	0.0044	0.843	0.11430	0.00108	1822	21	1869	17	2.5
7471-96.1	1	30 µm	72	164	2.346	38	1	4.78E-05	2.58E-05	0.0008	0.6760	0.0065	5.340	0.082	0.3382	0.0042	0.871	0.11452	0.00087	1878	20	1872	14	-0.3
7471-58.1	1	30 µm	56	63	1.170	23	2	1.08E-04	4.30E-05	0.0019	0.3398	0.0031	5.307	0.081	0.3346	0.0040	0.855	0.11502	0.00091	1861	19	1880	14	1
7471-31.1	1	30 µm	54	74	1.421	24	2	1.03E-04	4.25E-05	0.0018	0.4097	0.0031	5.366	0.075	0.3382	0.0037	0.856	0.11508	0.00084	1878	18	1881	13	0.2
7471-16.1	1	30 µm	73	21	0.300	26	2	9.56E-05	3.07E-05	0.0017	0.0859	0.0016	5.479	0.070	0.3421	0.0037	0.898	0.11616	0.00066	1897	18	1898	10	0.1
7471-47.1	1	15 µm	111	168	1.562	53	4	1.18E-04	5.91E-05	0.0020	0.4564	0.0057	5.719	0.099	0.3498	0.0042	0.769	0.11858	.00132	1933	20	1935	20	0.1
7471-47.2	1		94	107	1.172	39	0	1.05E-05	1.88E-05	0.0002	0.3318	0.0034	5.486	0.111	0.3344	0.0052	0.840	0.11898	0.00132	1860	25	1941	20	4.2
7471-28.1	1	30 µm	175	237	1.396	110	1	1.71E-05	8.86E-06	0.0003	0.3937	0.0018	10.692	0.121	0.4663	0.0050	0.979	0.16633	0.00038	2467	22	2521	4	2.1
7471-28.2	1	30 µm	115	117	1.051	72	0	5.08E-06	1.47E-05	0.0001	0.2914	0.0015	11.717	0.168	0.4968	0.0060	0.893	0.17107	0.00111	2600	26	2568	11	-1.2
z7475, granitic gneiss, Clearwater Domain																								
7475-63.1	2	30 µm	11	7	0.621	4	1	3.60E-04	1.76E-04	0.0062	0.1759	0.0088	5.071	0.210	0.3242	0.0071	0.629	0.11343	0.00368	1810	35	1855	60	2.4
7475-27.1	2	30 µm	21	13	0.622	8	2	3.00E-04	1.07E-04	0.0052	0.1974	0.0061	5.025	0.122	0.3210	0.0047	0.692	0.11354	0.00201	1795	23	1857	32	3.3
7475-101.1	2	30 µm	15	14	0.935	6	0	1.05E-04	1.34E-04	0.0018	0.2735	0.0071	5.622	0.165	0.3394	0.0051	0.613	0.12013	0.00281	1884	25	1958	42	3.8
7475-83.1	2	30 µm	22	9	0.440	8	1	1.50E-04	9.65E-05	0.0026	0.1230	0.0052	6.359	0.152	0.3540	0.0049	0.667	0.13028	0.00234	1954	23	2102	32	7
7475-12.1	2	30 µm	31	12	0.385	13	1	1.37E-04	4.85E-05	0.0024	0.1076	0.0029	6.936	0.122	0.3760	0.0044	0.751	0.13379	0.00156	2058	21	2148	21	4.2
7475-35.1	2	30 µm	37	16	0.439	16	2	1.74E-04	4.45E-05	0.0030	0.1167	0.0039	7.820	0.115	0.4017	0.0047	0.850	0.14120	0.00111	2177	21	2242	14	2.9
7475-3.3	1	30 µm	63	86	1.397	27	0	1.80E-05	3.96E-05	0.0003	0.4009	0.0041	5.321	0.108	0.3275	0.0050	0.831	0.12898	0.00123	2101	23	2084	17	-0.8
7475-94.2	1	30 µm	69	74	1.100	33	1	5.24E-05	3.63E-05	0.0009	0.3068	0.0049	6.852	0.116	0.3853	0.0050	0.831	0.14904	0.00110	2211	24	2335	13	5.3
7475-6.1	1	30 µm	113	70	0.641	53	1	2.45E-05	1.27E-05	0.0004	0.1809	0.0035	8.408	0.132	0.4092	0.0053	0.885	0.14904	0.00110	2211	24	2335	13	5.3
7475-98.1	1	30 µm	169	101	0.616	87	1	1.49E-05	8.62E-06	0.0003	0.1740	0.0012	9.545	0.341	0.4512	0.0053	0.439	0.15344	0.00496	2400	23	2385	56	-0.7
7475-14.2	1	30 µm	109	111	1.058	66	1	2.13E-05	1.11E-05	0.0004	0.2882	0.0020	10.493	0.159	0.4885	0.0056	0.830	0.15642	0.00133	2556	24	2417	15	-5.7
7475-85.2	1	30 µm	144	102	0.730	77	1	1.00E-05	1.00E-05	0.0002	0.2007	0.0013	9.924	0.268	0.4578	0.0051	0.510	0.15722	0.00366	2430	23	2426	40	-0.2
7475-85.1	1	15 µm	150	99	0.680	82	3	4.15E-05	2.41E-05	0.0007	0.1845	0.0026	10.394	0.161	0.4762	0.0057	0.840	0.15831	0.00134	2511	25	2438	14	-3
7475-43.1	1	30 µm	153	86	0.577	83	1	1.59E-05	8.90E-06	0.0003	0.1611	0.0013	10.618	0.163	0.4765	0.0056	0.833	0.16162	0.00138	2512	24	2473	15	-1.6
7475-3.1	1	15 µm	119	81	0.698	62	0	1.00E-05	1.00E-05	0.0002	0.1958	0.0033	9.950	0.163	0.4443	0.0053	0.808	0.16244	0.00158	2370	24	2481	17	4.5
7475-3.2	1	30 µm	122	81	0.684	68	0	1.33E-05	1.40E-05	0.0000	0.1935	0.0056	10.787	0.462	0.4812	0.0134	0.736	0.16258	0.00475	2533	59	2483	50	-2
7475-72.1	1	30 µm	71	75	1.085	41	1	4.51E-05	1.51E-05	0.0008	0.3032	0.0037	10.379	0.178	0.4618	0.0063	0.863	0.16300	0.00142	2448	28	2487	15	1.6
7475-34.1	1	30 µm	208	119	0.591	116	1	1.00E-05	1.00E-05	0.0002	0.1664	0.0012	11.064	0.240	0.4861	0.0055	0.620	0.16509	0.00283	2554	24	2508	29	-1.8
7475-2.1	1	30 µm	199	115	0.603	112	0	2.06E-06	5.33E-06	0.0000	0.1658	0.0019	11.224	0.218	0.4921	0.0071	0.812	0.16543	0.00189	2580	31	2512	19	-2.7

Table 1. (cont.)

Spot name	Zircon generation (see text)	Spot size	U (ppm)	Th (ppm)	Th/U	Pb* (ppm)	^{204}Pb (ppb)	$^{204}Pb/^{206}Pb$	± $^{204}Pb/^{206}Pb$	f(206)^{204}	$^{206*}Pb/^{238*}Pb$	± $^{206}Pb/^{238}U$	$^{207*}Pb/^{235*}U$	± $^{207}Pb/^{235}U$	$^{206*}Pb/^{238}U$	± $^{206}Pb/^{238}U$	Corr Coeff	$^{207*}Pb/^{206*}Pb$	± $^{207}Pb/^{206}Pb$	Apparent ages (Ma) $^{206}Pb/^{238}U$	± $^{206}Pb/^{238}U$	$^{207}Pb/^{206}Pb$	± $^{207}Pb/^{206}Pb$	Disc. (%)
7475-94.1	1	30 µm	224	128	0.592	122	1	6.76E-06	8.91E-06	0.0001	0.1687	0.0015	10.845	0.346	0.4718	0.0050	0.447	0.16672	0.00480	2491	22	2525	49	1.3
7475-14.1	1	30 µm	133	74	0.574	73	0	6.78E-06	9.11E-06	0.0001	0.1608	0.0011	11.052	0.141	0.4776	0.0051	0.896	0.16782	0.00096	2517	22	2536	10	0.8
z7477, Maybelle granodiorite																								
7477-59.1	3	15 µm	621	119	0.196	218	1	7.93E-06	5.88E-06	0.0001	0.0570	0.0008	5.755	0.072	0.3472	0.0037	0.914	0.12021	0.00061	1921	18	1959	9	1.9
7477-7.1	2	15 µm	3597	8052	2.313	1906	9	8.15E-06	2.54E-06	0.0001	0.6695	0.0023	5.589	0.087	0.3438	0.0051	0.977	0.11793	0.00039	1905	24	1925	6	1.1
7477-62.1	2	15 µm	147	65	0.460	54	1	2.84E-05	2.73E-05	0.0005	0.1341	0.0024	5.553	0.087	0.3401	0.0043	0.876	0.11841	0.00090	1887	21	1932	14	2.3
7477-91.1	2	30 µm	285	87	0.317	105	1	7.25E-06	8.11E-06	0.0001	0.0924	0.0011	5.848	0.085	0.3526	0.0043	0.900	0.12028	0.00077	1947	21	1960	11	0.7
7477-62.2	2	15 µm	182	77	0.437	67	1	1.00E-05	1.00E-05	0.0002	0.1298	0.0021	5.643	0.086	0.3402	0.0045	0.924	0.12030	0.00071	1888	22	1961	11	3.7
7477-18.2	2	15 µm	1963	529	0.278	669	3	5.01E-06	2.76E-06	0.0001	0.0797	0.0007	5.481	0.068	0.3302	0.0036	0.928	0.12039	0.00056	1839	17	1962	8	6.3
7477-81.1	2	15 µm	201	169	0.866	79	2	3.96E-05	1.83E-05	0.0007	0.2495	0.0035	5.574	0.097	0.3351	0.0047	0.867	0.12062	0.00106	1863	23	1965	16	5.2
7477-70.2	2	30 µm	675	236	0.361	249	2	9.73E-06	3.67E-06	0.0002	0.1036	0.0006	5.821	0.074	0.3499	0.0040	0.940	0.12064	0.00053	1934	19	1966	8	1.6
7477-74.1	2	15 µm	2783	1085	0.401	1003	1	1.82E-06	1.86E-06	0.0000	0.1162	0.0009	5.622	0.063	0.3375	0.0036	0.972	0.12081	0.00032	1875	17	1968	5	4.7
7477-102.1	2	30 µm	2182	634	0.300	763	1	1.24E-06	1.29E-06	0.0000	0.0871	0.0003	5.609	0.083	0.3364	0.0048	0.987	0.12094	0.00029	1869	23	1970	4	5.1
7477-81.2	2	15 µm	191	100	0.544	72	1	2.23E-05	3.32E-05	0.0004	0.1543	0.0027	5.714	0.082	0.3422	0.0041	0.886	0.12110	0.00081	1897	20	1972	12	3.8
7477-15.2	2	15 µm	356	255	0.740	133	4	4.37E-05	1.22E-05	0.0008	0.2138	0.0036	5.427	0.067	0.3248	0.0035	0.927	0.12117	0.00057	1813	17	1974	8	8.1
7477-18.1	2	15 µm	1617	473	0.302	590	1	2.71E-06	3.13E-06	0.0001	0.0867	0.0006	5.866	0.073	0.3510	0.0039	0.943	0.12121	0.00051	1939	19	1974	7	1.8
7477-70.1	2	15 µm	961	68	0.073	332	3	1.00E-05	1.00E-05	0.0002	0.0207	0.0005	5.886	0.084	0.3514	0.0040	0.867	0.12148	0.00087	1941	19	1978	13	1.9
7477-102.2	2	30 µm	2391	841	0.363	823	3	4.02E-06	1.12E-06	0.0001	0.1046	0.0003	5.474	0.063	0.3264	0.0036	0.982	0.12165	0.00027	1821	17	1981	4	8.1
7477-15.1	2	15 µm	447	220	0.508	170	1	5.21E-06	8.93E-06	0.0001	0.1486	0.0015	5.852	0.073	0.3477	0.0039	0.943	0.12208	0.00051	1923	19	1987	7	3.2
7477-45.1	2	15 µm	170	92	0.559	64	0	1.00E-05	1.00E-05	0.0002	0.1605	0.0022	5.756	0.096	0.3419	0.0050	0.926	0.12209	0.00077	1896	24	1987	11	4.6
7477-70.3	2	30 µm	640	237	0.383	227	1	8.00E-06	4.91E-06	0.0001	0.1093	0.0008	5.663	0.076	0.3345	0.0039	0.920	0.12278	0.00065	1860	19	1997	9	6.9
7477-12.1	1	15 µm	4357	1740	0.413	1658	37	2.76E-05	2.97E-06	0.0005	0.1196	0.0006	6.219	0.072	0.3547	0.0039	0.971	0.12716	0.00035	1957	18	2059	5	5
7477-49.1	1	15 µm	516	187	0.375	201	1	8.10E-06	7.81E-06	0.0001	0.1047	0.0014	6.481	0.087	0.3678	0.0044	0.928	0.12779	0.00065	2019	21	2068	9	2.3
7477-3.1	1	15 µm	484	174	0.372	196	2	1.00E-05	1.00E-05	0.0002	0.1055	0.0010	7.018	0.095	0.3810	0.0048	0.967	0.13359	0.00047	2081	23	2146	6	3
7477-26.2	1	15 µm	2427	835	0.355	1010	3	3.88E-06	1.45E-06	0.0001	0.1009	0.0006	7.711	0.102	0.3887	0.0046	0.933	0.14387	0.00069	2117	21	2274	8	6.9
7477-8.1	1	15 µm	257	187	0.752	121	1	1.57E-05	1.47E-05	0.0003	0.2155	0.0023	7.976	0.150	0.4017	0.0068	0.940	0.14402	0.00093	2177	31	2276	11	4.4
z7478, Fishing Creek quartz diorite																								
7478-80.1	3	15 µm	1085	81	0.077	378	3	1.00E-05	1.00E-05	0.0002	0.0216	0.0006	5.885	0.074	0.3551	0.0039	0.928	0.12021	0.00057	1959	19	1959	8	0
7478-57.2	2	15 µm	447	39	0.090	150	2	1.69E-05	1.11E-05	0.0003	0.0256	0.0007	5.555	0.071	0.3421	0.0039	0.942	0.11777	0.00051	1897	19	1923	8	1.3
7478-79.1	2	15 µm	727	18	0.026	241	2	1.16E-05	7.11E-06	0.0002	0.0078	0.0004	5.586	0.061	0.3422	0.0035	0.963	0.11840	0.00036	1897	17	1932	5	1.8
7478-48.1	2	15 µm	394	74	0.194	135	0	1.59E-06	1.30E-05	0.0000	0.0561	0.0010	5.578	0.076	0.3399	0.0040	0.911	0.11903	0.00067	1886	19	1942	10	2.9
7478-42.1	2	15 µm	690	308	0.460	264	2	7.14E-06	8.09E-06	0.0001	0.1323	0.0012	5.841	0.076	0.3555	0.0043	0.960	0.11916	0.00044	1961	20	1944	7	-0.9
7478-72.1	2	15 µm	92	35	0.394	33	0	1.00E-05	1.00E-05	0.0002	0.1173	0.0026	5.524	0.090	0.3347	0.0044	0.872	0.11972	0.00096	1861	21	1952	14	4.7
7478-52.2	2	15 µm	606	316	0.538	234	2	1.00E-05	1.00E-05	0.0002	0.1580	0.0013	5.804	0.069	0.3512	0.0037	0.938	0.11986	0.00050	1940	18	1954	7	0.7
7478-52.1	2	15 µm	611	420	0.709	242	4	2.10E-05	7.54E-06	0.0004	0.2027	0.0015	5.750	0.068	0.3478	0.0037	0.944	0.11992	0.00047	1924	18	1955	7	1.6
7478-63.2	2	15 µm	879	277	0.326	319	3	1.00E-05	1.00E-05	0.0002	0.0935	0.0008	5.759	0.066	0.3482	0.0037	0.958	0.11997	0.00040	1926	18	1956	6	1.5
7478-15.1	2	15 µm	559	226	0.418	207	1	6.43E-06	7.67E-06	0.0001	0.1198	0.0021	5.735	0.084	0.3462	0.0041	0.875	0.12013	0.00086	1917	20	1958	13	2.1
7478-49.1	2	15 µm	192	62	0.332	71	0	2.50E-07	2.27E-05	0.0000	0.0961	0.0019	5.874	0.087	0.3533	0.0043	0.883	0.12059	0.00085	1950	21	1965	13	0.7
7478-15.2	2	15 µm	620	405	0.675	250	2	1.00E-05	1.00E-05	0.0002	0.1934	0.0031	5.934	0.073	0.3568	0.0039	0.928	0.12062	0.00056	1967	18	1966	8	-0.1
7478-28.1	2	15 µm	637	482	0.782	261	4	1.83E-05	6.79E-06	0.0003	0.2291	0.0016	5.867	0.075	0.3525	0.0038	0.903	0.12072	0.00067	1947	18	1967	10	1
7478-99.1	2	15 µm	373	199	0.552	142	1	1.00E-05	1.00E-05	0.0002	0.1602	0.0017	5.741	0.082	0.3447	0.0042	0.908	0.12080	0.00073	1909	20	1968	11	3
7478-86.1	2	15 µm	326	142	0.450	123	1	1.00E-05	1.00E-05	0.0002	0.1299	0.0015	5.842	0.076	0.3501	0.0041	0.938	0.12102	0.00055	1935	19	1971	8	1.8
7478-68.1	2	15 µm	696	386	0.574	268	2	1.00E-05	1.00E-05	0.0002	0.1662	0.0023	5.802	0.073	0.3476	0.0040	0.948	0.12104	0.00049	1923	19	1972	7	2.5
7478-71.1	2	15 µm	477	269	0.583	186	4	3.11E-05	9.24E-06	0.0005	0.1674	0.0014	5.876	0.070	0.3519	0.0038	0.943	0.12109	0.00048	1944	18	1972	7	1.4
7478-53.1	2	15 µm	751	273	0.376	280	1	3.60E-06	8.52E-06	0.0001	0.1089	0.0010	5.888	0.074	0.3522	0.0039	0.935	0.12126	0.00055	1945	19	1975	8	1.5
7478-36.1	2	15 µm	612	207	0.350	226	2	1.00E-05	1.00E-05	0.0002	0.1045	0.0011	5.871	0.071	0.3509	0.0039	0.955	0.12136	0.00044	1939	19	1976	6	1.9
7478-53.2	2	15 µm	666	258	0.400	246	2	1.00E-05	1.00E-05	0.0002	0.1170	0.0014	5.796	0.084	0.3463	0.0042	0.889	0.12139	0.00081	1917	20	1977	12	3
7478-64.1	2	15 µm	556	189	0.351	205	3	1.99E-05	1.07E-05	0.0003	0.1018	0.0020	5.864	0.077	0.3503	0.0039	0.905	0.12142	0.00068	1936	19	1977	10	2.1
7478-6.1	2	15 µm	604	332	0.569	231	0	1.33E-06	6.45E-06	0.0000	0.1632	0.0034	5.812	0.071	0.3456	0.0038	0.951	0.12197	0.00047	1914	18	1985	7	3.6
7478-63.1	1	15 µm	73	34	0.485	27	0	1.00E-05	1.00E-05	0.0002	0.1407	0.0033	5.586	0.112	0.3412	0.0053	0.837	0.11873	0.00131	1892	25	1937	20	2.3
7478-81.2	1	15 µm	134	84	0.645	51	0	1.00E-05	1.00E-05	0.0002	0.1952	0.0035	5.565	0.097	0.3326	0.0043	0.824	0.12135	0.00120	1851	21	1976	18	5.3
7478-17.1	1	15 µm	269	36	0.139	94	1	9.42E-06	1.43E-05	0.0002	0.0417	0.0010	5.905	0.078	0.3479	0.0038	0.879	0.12312	0.00079	1924	18	2002	11	3.9
7478-81.1	1	15 µm	158	102	0.666	61	3	6.38E-05	2.52E-05	0.0011	0.1961	0.0027	5.800	0.095	0.3396	0.0048	0.912	0.12387	0.00084	1885	23	2013	12	6.4
7478-32.1	1	15 µm	337	176	0.540	157	6	5.04E-05	1.94E-05	0.0009	0.1593	0.0033	8.438	0.114	0.4151	0.0047	0.887	0.14743	0.00093	2238	21	2316	11	3.4

Notes (see Stern, 1997)

Uncertainties reported at 1σ (absolute) and are calculated by numerical propagation of all known sources of error

f(206)^{204} refers to mole fraction of total ^{206}Pb that is due to common Pb, calculated using the ^{204}Pb-method; common Pb composition used is the surface blank

Discordance relative to origin = 100 * (1-(^{206}Pb/^{238}U age)/(^{207}Pb/^{206}Pb age))

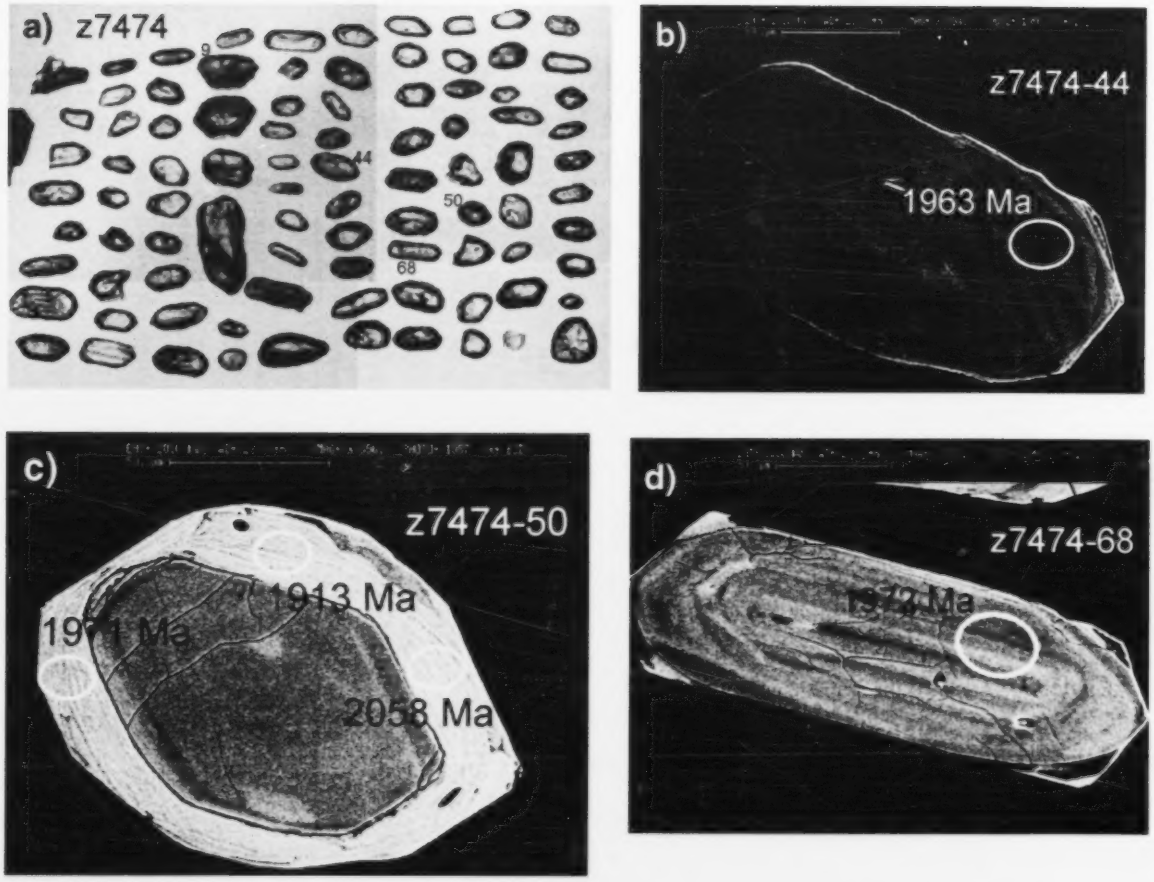

Figure 3. *Zircons from z7474, aplitic granite, Virgin River shear zone;* ***a)*** *transmitted light,* ***b)–d)*** *back-scattered electrons. Ellipses show locations of SHRIMP analysis sites and* $^{207}Pb/^{206}Pb$ *dates.*

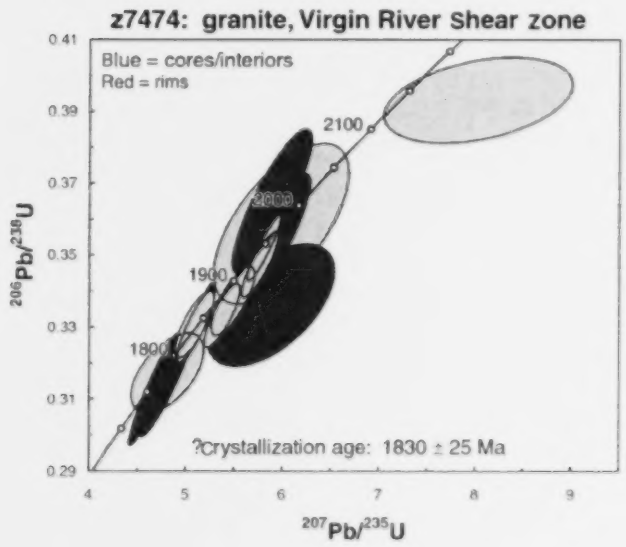

Figure 4.

SHRIMP U-Pb zircon results for z7474, aplitic granite, Virgin River shear zone.

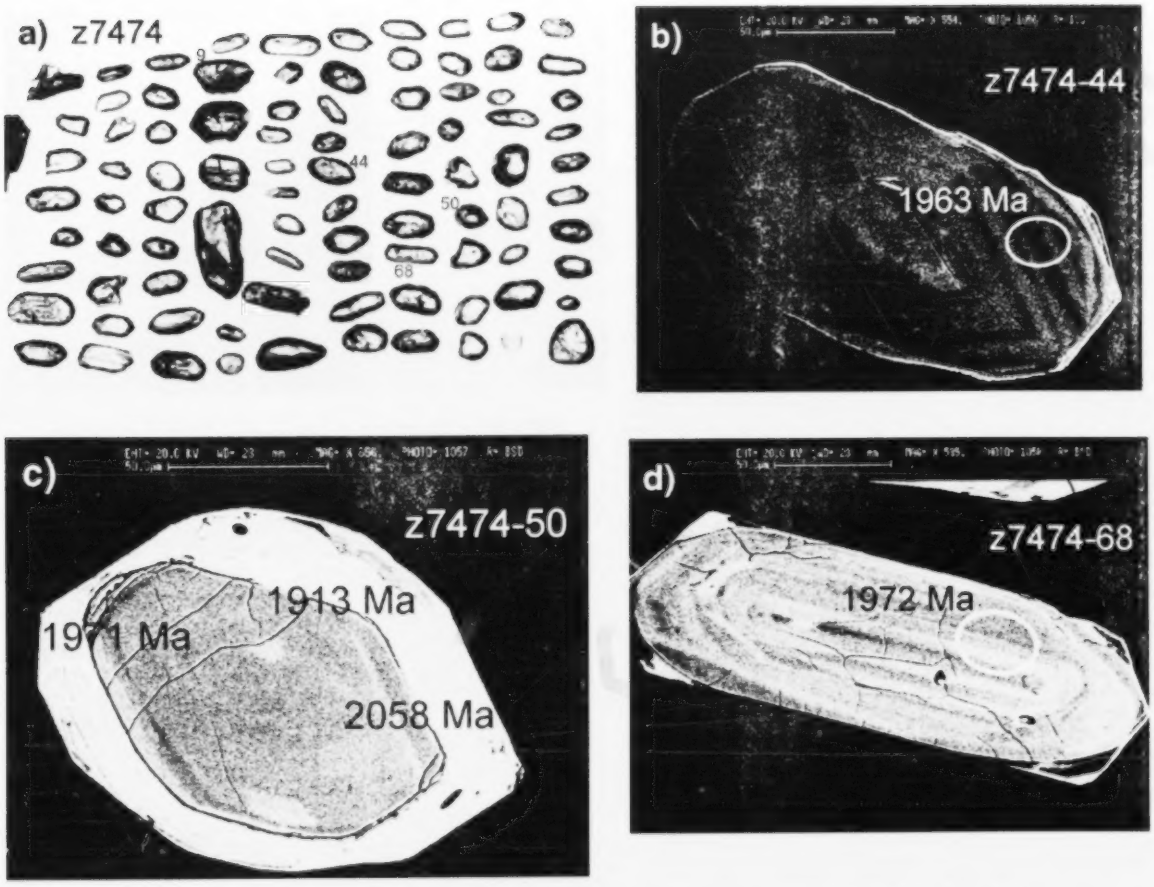

Figure 3. *Zircons from z7474, aplitic granite, Virgin River shear zone: **a)** transmitted light, **b)–d)** back-scattered electrons. Ellipses show locations of SHRIMP analysis sites and $^{207}Pb/^{206}Pb$ dates.*

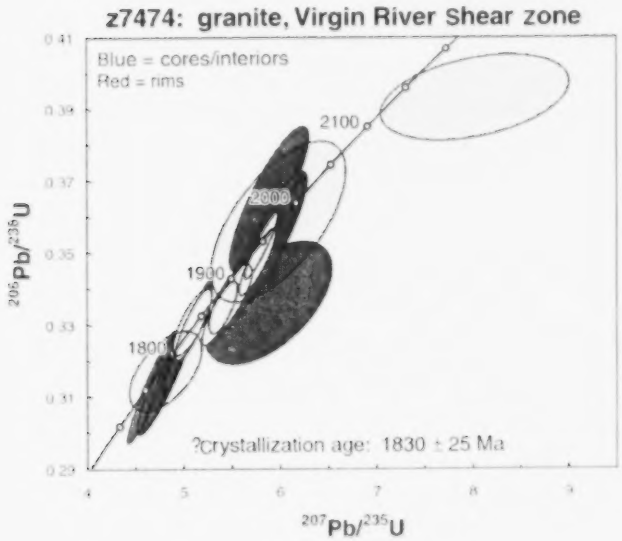

Figure 4.

SHRIMP U-Pb zircon results for z7474, aplitic granite, Virgin River shear zone.

Table 2. Summary of SHRIMP U-Pb zircon ages for granitoid basement samples beneath the southern and southwestern portions of the Athabasca Basin.

GSC Sample #	Field #	UTM	Unit	Domain	Crystallization age (Ma)	Inheritance ages (Ga)	Metamorphism (Ma)
7474	0261-59	12,661271, 6348900	Aplitic granite	Virgin River	ca1830*	1.9–2.3	
7472	0261-5	12,658776, 6352060	Quartz diorite	E. Lloyd/Taltson	1985 ± 11 (?1948*)	2.1–2.4	1941 ± 24, 1897 ± 8
7473	0261-7	12,658009, 6352092	Leucogranite	E. Lloyd/Taltson	1975 ± 5	>2.0	1927 ± 34
7471	0261-184	12,589403, 6326127	Granite	Clearwater	1843 ± 4	1.87, 1.94, 2.55	1822 ± 12
7475	0261-186	12,594058, 6321713	Granitic gneiss xenolith	Clearwater	ca. 2500*		1856 ± 56
7477	3502	12,551150, 6408404	Maybelle granodiorite	W. Lloyd/Taltson	1974 ± 5	2.06–2.28	
7478	3503	12,482537, 6470886	Fishing Creek quartz diorite	W. Lloyd/Taltson	1968 ± 5	2.0–2.3	

* *see* text for discussion

to planar-banded zoning, with the thin (about 10 µm wide) outer rims appearing very bright. The rim zircon is faintly oscillatory zoned in places (e.g. Fig. 3c).

B) Irregular (100–200 µm diameter), anhedral grains and grain fragments are the second type. Some of these grains also have faint outer rim growths, whereas others look resorbed, having rounded grain edges. Backscattered electron images are similar to those of zircon type A.

A total of 16 spot dates were obtained from 12 grains (Fig. 4). Data from cores and interiors of grains with banded zoning are concordant to slightly discordant, with $^{207}Pb/^{206}Pb$ dates ranging from 2324 Ma to 1804 Ma (Fig. 4). Three analyses of the central portion of grain 9, a large prismatic grain comprising dominantly faint planar-banded zoning in its interior overgrown by a thin rim (Fig. 3a), yielded $^{207}Pb/^{206}Pb$ dates between 1837 Ma to 1804 Ma, with a weighted mean of 1832 ± 22 Ma (MSWD = 0.26, P = 0.77). Uranium concentrations for grain interiors are 40 ppm to 150 ppm, and Th/U ratios show a wide range, 0.01–2. Clearly, the large age range and geochemical diversity indicates that the zircons are of diverse origins, including likely igneous and inherited populations.

Zircon rims were targeted in seven locations (five grains) where they were sufficiently wide for analysis. The $^{207}Pb/^{206}Pb$ dates range from 2058 Ma to 1775 Ma and are less than 10% discordant (Fig. 4). Uranium concentrations are from 650–1800 ppm and Th/U rations from 0.02–0.2. A bright oscillatory zoned rim on grain 50 (Fig. 3c) yielded three spots with dates of 2058 Ma, 1971 Ma, and 1913 Ma, yielding a weighted mean of 1953 ± 120 Ma (MSWD = 2.6; P = 0.074). For the remaining four analyses, a weighted mean yields 1812 ± 39 Ma (MSWD = 4.3, P = 0.005); excluding the 1775 Ma date (?Pb-loss) yields 1823 ± 13 Ma (MSWD = 0.96, P = 0.38). The range of ages for the rims suggests complications in terms of Pb loss or partial incorporation of inherited radiogenic Pb.

If the rims are dominantly of metamorphic in origin, as evidenced by their generally low Th/U, then it is likely that the rock is older than 1823 Ma, the apparent age of one such rim. On the other hand, if all the zircon in the cores is inherited, then a maximum age for the rock is the 1832 Ma age of grain 9. It is also conceivable that grain 9 represents entirely igneous growth. Given the lack of clearly defined age modes, it is suggested that the crystallization age is probably around 1830 Ma, with an estimated uncertainity of ±25 Ma.

z7472 (quartz diorite, eastern Lloyd Domain)

The zircons recovered comprise several morphological types (Fig. 5).

A) The first type is brown, highly fractured prisms, typically 75 µm across and aspect ratios of 2–4:1, moderately clear to highly turbid, rounded grain edges, with some core-overgrowth features, particularly brown-turbid cores with clear overgrowths (possibly type D; *see* below). In BSE images, these grains have bright and finely oscillatory-zoned interiors, and most are variably resorbed and overgrown by dark BSE images, featureless zircon. Some interior parts of these grains display weakly zoned, relatively dark BSE images of zircon, suggesting an older generation within the fine-oscillatory zircon, but there are no obvious structural breaks. Other interior parts are bright and faintly zoned BSE images, but without clearly defined oscillatory zoning.

B) The second type is equant, multifaceted euhedral to anhedral and generally rounded grains, 75–200 µm diameter, clear, with few fractures or inclusions, and colourless. A few grains are stubby prisms. In BSE images, these are uniformly dark, unzoned, and about half possess a faintly oscillatory-zoned remnant core with bright BSE response.

C) Zircon fragments, pale pink-orange, clear, without cracks or inclusions defines the third type. They are dark in BSE images, and are faintly planar banded or show nebulous zoning.

D) The fourth type is semi-hemispheres of clear, colourless zircon that are likely to be broken off outer shells of more complex grains (e.g. grain 51, Fig. 5a). In BSE images they are uniformly dark.

Four generations of zircon growth are recognized. Generation 1 comprises diffusely zoned interiors of zircon morphological types A and B, and is interpreted as remnants of inherited zircon. An example of generation 1 zircon core occurring within type A morphology is shown in Figure 5b.

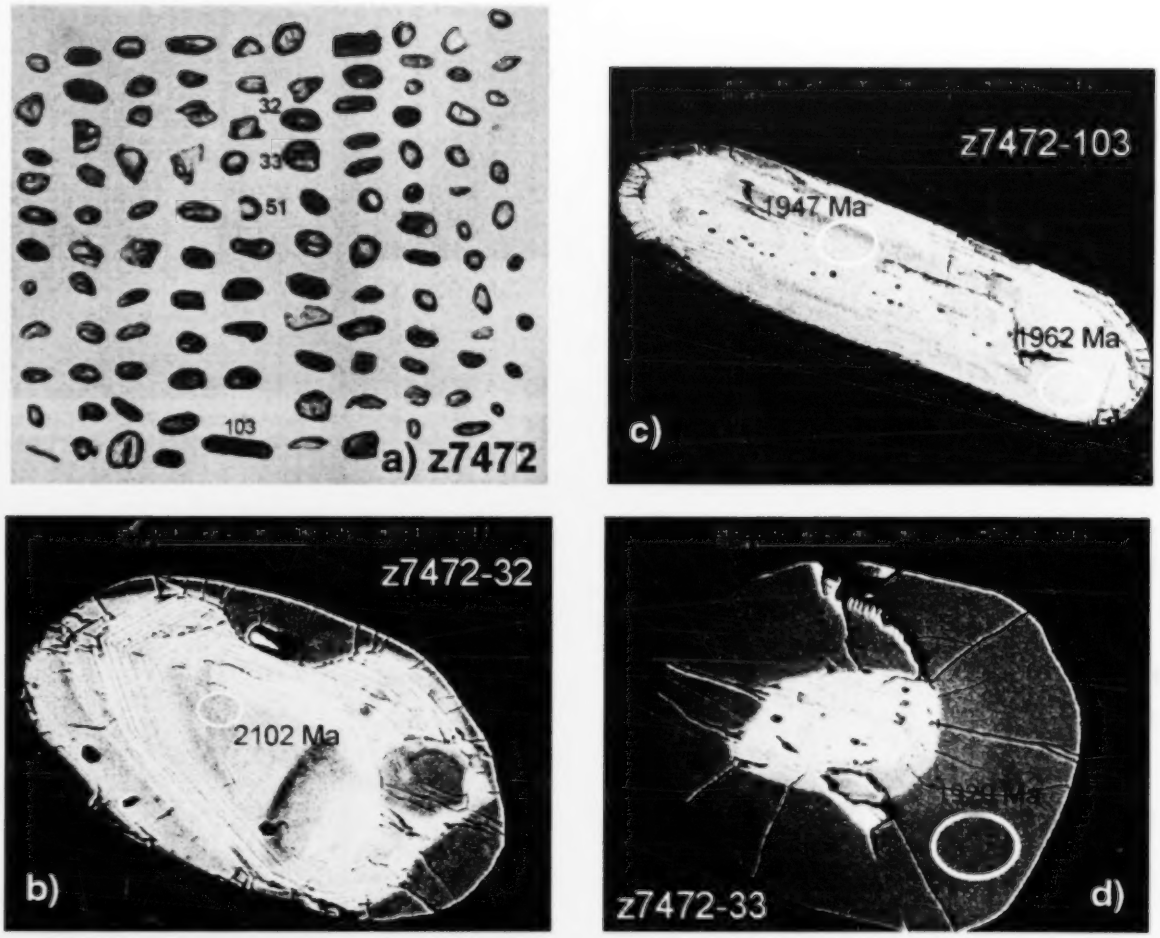

Figure 5. *Zircons from z7472, quartz diorite, eastern Lloyd Domain;* ***a)*** *transmitted light,* ***b)–d)*** *backscattered electrons. Ellipses show locations of SHRIMP analysis sites and* $^{207}Pb/^{206}Pb$ *dates.*

Generation 2 comprises dominantly oscillatory zircon within morphological types A and B that likely represents the main igneous growth of the protolith. Examples of generation 2 oscillatory zircon occurring with the type A morphology are shown in Figure 5b and 5c, and within type B in Figure 5d. Generation 3 zircon comprises uniformly dark BSE response zircon found within morphological types A, B, and D, and likely represents metamorphic growth. This zircon generation dominates type B zircon, as illustrated in Figure 5d. Generation 4 zircon is found exclusively in type C morphology and apparently represents separate fragments of the youngest zircon (*see* below).

A total of 33 SHRIMP analyses were obtained from 27 grains (Fig. 6). Four analyses of generation 1 zircon spread along and slightly below concordia, and have $^{207}Pb/^{206}Pb$ dates ranging from 2412 Ma to 2102 Ma. There are insufficient data to distinguish whether the data represent a single population of inherited zircon that has suffered ancient Pb loss, or the presence of multiple generations of inheritance. Uranium contents are typically around 250 ppm, with Th/U about 0.5.

Analyses of generation 2 magmatic zircon (n = 18) are concordant, having $^{207}Pb/^{206}Pb$ dates of 2012–1915 Ma, but do not define a single population (inset, Fig. 6). The U contents are 300–900 ppm, and Th/U = 0.2–1.0. On a relative probability curve (Fig. 6), the data define three modes. The youngest mode comprises two analyses with a mean date of 1917 Ma. The majority (n = 10) of analyses occupying the central peak have a weighted mean age of 1948 ± 7 (MSWD = 1.2; P = 29%). The six analyses from four different grains making up the oldest mode have $^{207}Pb/^{206}Pb$ dates of 2012–1973 Ma, with a weighted mean of 1990 ± 14 Ma (MSWD = 3.1; P = 0.8%). Eliminating the oldest analysis from generation 2, as a possibly unrecognized inheritance date, yields 1985 ± 11 Ma (MSWD = 1.3; P = 25%). This latter date is taken as the most likely age of crystallization,

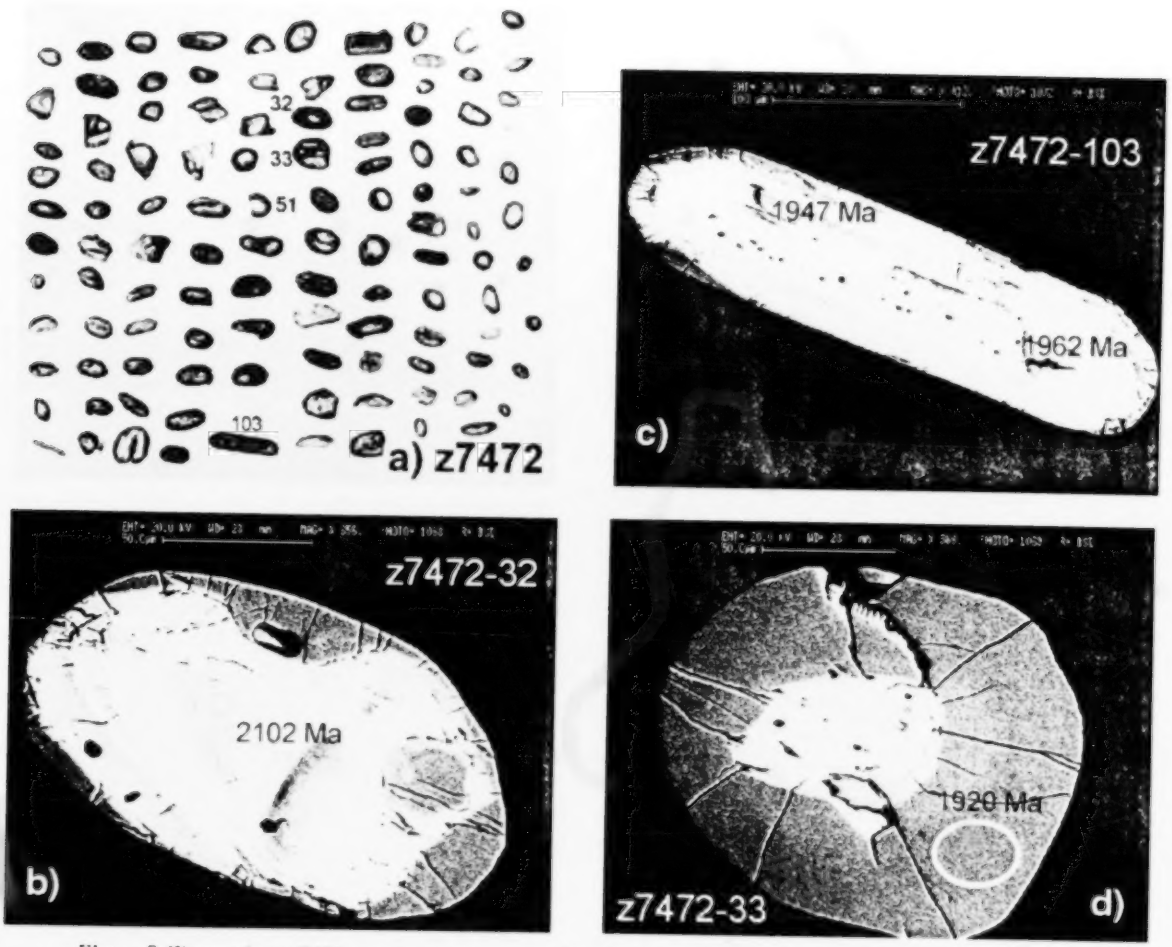

Figure 5. *Zircons from z7472, quartz diorite, eastern Lloyd Domain:* ***a)*** *transmitted light,* ***b)–d)*** *backscattered electrons. Ellipses show locations of SHRIMP analysis sites and $^{207}Pb/^{206}Pb$ dates.*

Generation 2 comprises dominantly oscillatory zircon within morphological types A and B that likely represents the main igneous growth of the protolith. Examples of generation 2 oscillatory zircon occurring with the type A morphology are shown in Figure 5b and 5c, and within type B in Figure 5d. Generation 3 zircon comprises uniformly dark BSE response zircon found within morphological types A, B, and D, and likely represents metamorphic growth. This zircon generation dominates type B zircon, as illustrated in Figure 5d. Generation 4 zircon is found exclusively in type C morphology and apparently represents separate fragments of the youngest zircon (*see* below).

A total of 33 SHRIMP analyses were obtained from 27 grains (Fig. 6). Four analyses of generation 1 zircon spread along and slightly below concordia, and have $^{207}Pb/^{206}Pb$ dates ranging from 2412 Ma to 2102 Ma. There are insufficient data to distinguish whether the data represent a single population of inherited zircon that has suffered ancient Pb loss, or the presence of multiple generations of inheritance. Uranium contents are typically around 250 ppm, with Th/U about 0.5.

Analyses of generation 2 magmatic zircon (n = 18) are concordant, having $^{207}Pb/^{206}Pb$ dates of 2012–1915 Ma, but do not define a single population (inset, Fig. 6). The U contents are 300–900 ppm, and Th/U = 0.2–1.0. On a relative probability curve (Fig. 6), the data define three modes. The youngest mode comprises two analyses with a mean date of 1917 Ma. The majority (n = 10) of analyses occupying the central peak have a weighted mean age of 1948 ± 7 (MSWD = 1.2; P = 29%). The six analyses from four different grains making up the oldest mode have $^{207}Pb/^{206}Pb$ dates of 2012–1973 Ma, with a weighted mean of 1990 ± 14 Ma (MSWD = 3.1; P = 0.8%). Eliminating the oldest analysis from generation 2, as a possibly unrecognized inheritance date, yields 1985 ± 11 Ma (MSWD = 1.3; P = 25%). This latter date is taken as the most likely age of crystallization.

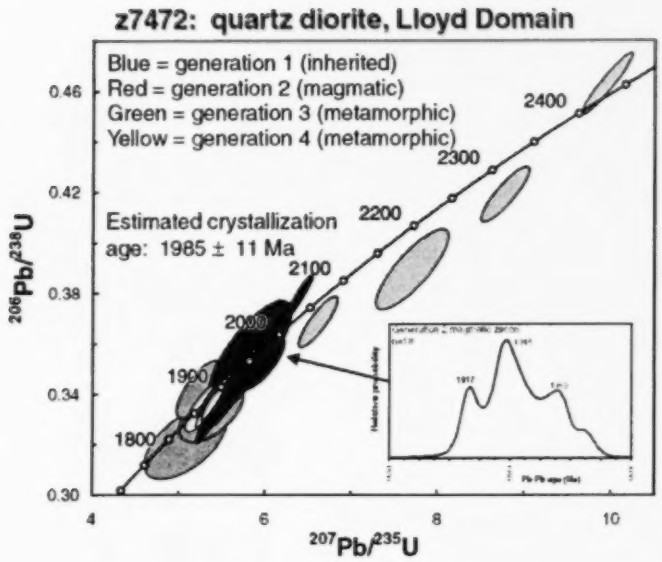

Figure 6.

SHRIMP U-Pb zircon results for z7472, quartz diorite, eastern Lloyd Domain. Inset shows a cumulative probability curve for generation 2 magmatic zircon.

although the prominence of the 1948 Ma mode makes it conceivable that this could instead represent the crystallization age, with the older dates being affected by inheritance.

Generation 3 zircon is characterized by low U (11–32 ppm) and Th/U of 0.1–0.5. The analytical uncertainties are relatively large owing to the low U, but the U-Pb results (n = 6) are within 5% of concordia and have $^{207}Pb/^{206}Pb$ dates of 1967 Ma to 1820 Ma. Excluding the youngest analysis, the weighted mean of five spots is 1941 ± 24 Ma (MSWD = 1.4; P = 24%), which is taken as an age of high-grade metamorphism recorded in the eastern Lloyd Domain.

Generation 4 fragments have U contents of 30–100 ppm and Th/U of about 0.2. Five concordant analyses have $^{207}Pb/^{206}Pb$ dates of 1902 Ma to 1876 Ma, with a weighted mean of 1897 ± 8 Ma (MSWD = 0.56; P = 69%). This result indicates that a second metamorphic event affected the rock.

z7473 (leucogranite, eastern Lloyd Domain)

Two morphological types of zircon are recognized from this sample (Fig. 7).

A) The first type is large (100–150 µm wide; l:w = 2–3:1), pale pink-brown prisms, with rounded grain edges, prominent fracturing, and minor clear inclusions. Some obvious structural cores are visible in reflected light. Backscattered electron images reveal bright, unzoned, or faintly banded to finely oscillatory-zoned zircon. A few structural cores are present that are bright in BSE images, but most are strongly altered and dull in BSE images. Most grains have an unzoned outer rim that is slightly darker in BSE images.

B) The second type is equant to stubby prismatic grains, 75–150 µm diameter, some with multifaceting, and others subrounded. Backscattered electron images are unzoned or show faint banded or weak sector zoning

Three generations of zircon growth are recognized. Generation 1 zircon comprises inherited zircon, and appears to be very minor. Magmatic zircon of generation 2 comprises most of the zircon making up both morphological types A and B. Examples of generation 2 growth in type A zircon can be seen in Figure 7b and 7c as the dominant areas of bright zircon, and in type B zircon in Figure 7d (grains 34, 36), where it appears as broadly and diffusely zoned. Structural cores such as shown in Figure 7b (grain 46) are also of generation 2 age. Zircon of generation 3 is present mainly in type A grains as thin rims, as clearly evident in Figure 7b and 7c, and is thought to be of metamorphic origin.

A total of 35 analyses were acquired from 29 grains (Fig. 8). None of the obvious structural cores, such as the one shown in Figure 7b (grain 46) proved to have dates indicative of inheritance; however, a single analysis of the central part of a type B rounded zircon (7473-15.1; Table 1) is 9% discordant and has a $^{207}Pb/^{206}Pb$ date of 2049 Ma. (Fig. 8). Despite the absence of obvious internal structures in this grain, the date is interpreted as being influenced by inheritance, with likely mixing with magmatic zircon of generation 2.

Thirty-three analyses of generation 2 zircon from type A and B zircons are all nearly concordant (Fig. 8), with U from 250–750 ppm and Th/U varying from 0.1–0.7. The $^{207}Pb/^{206}Pb$ dates range from 1997 Ma to 1901 Ma. The distribution of data on a relative probability curve (inset, Fig. 8) are negatively skewed, with a major peak at ca. 1972 Ma, consistent with variable extents of Pb-loss from a single original age. The weighted mean of the 18 oldest analyses is 1975 ± 5 (MSWD = 1.4; P = 14%), which is considered the crystallization age.

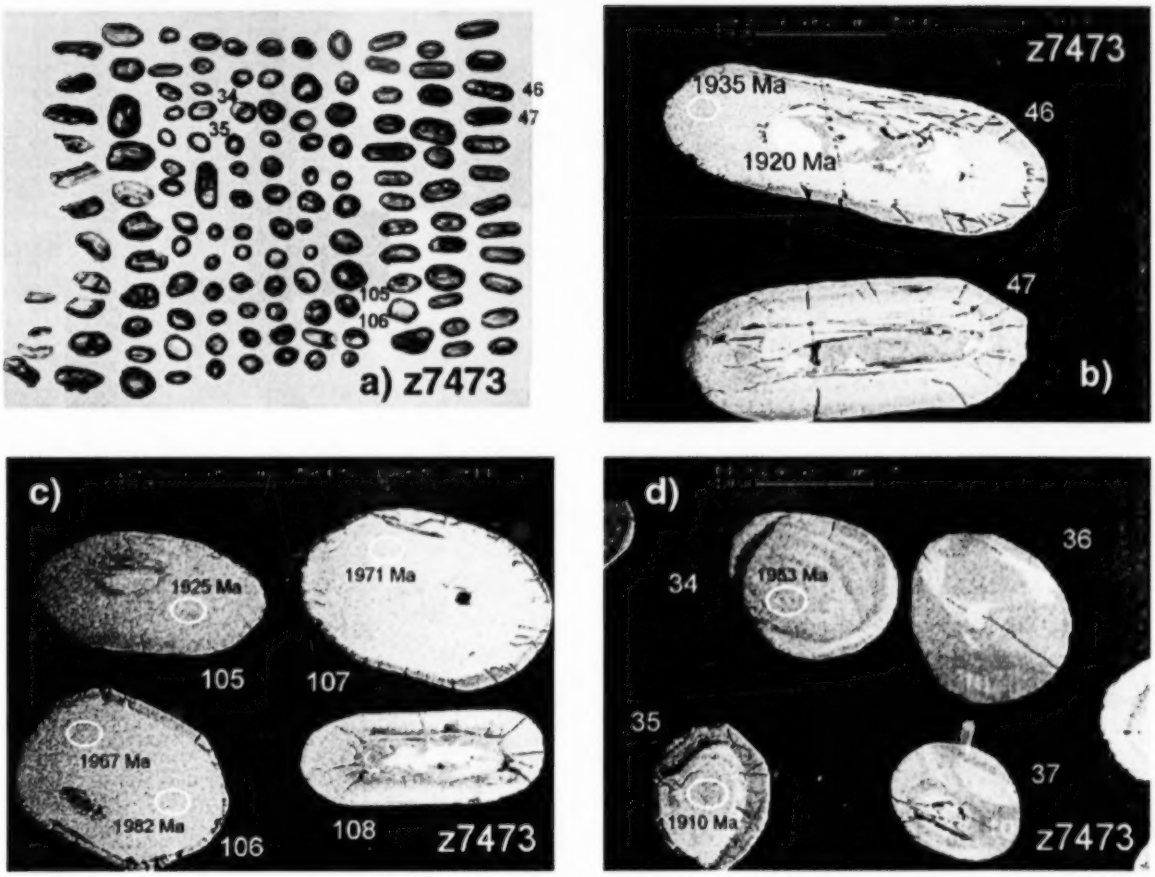

Figure 7. *Zircons from z7473, leucogranite, eastern Lloyd Domain;* ***a)*** *transmitted light,* ***b)–d)*** *backscattered electrons. Ellipses show locations of SHRIMP analysis sites and $^{207}Pb/^{206}Pb$ dates.*

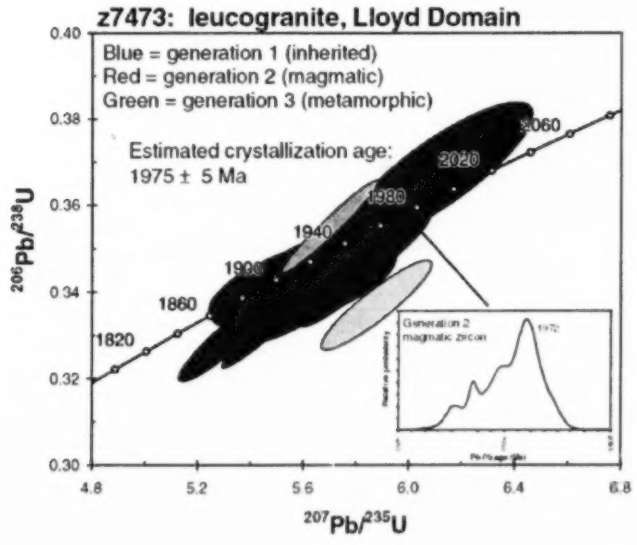

Figure 8.

SHRIMP U-Pb zircon results for z7473, leucogranite, eastern Lloyd Domain. Inset shows a cumulative probability curve for generation 2 magmatic zircon.

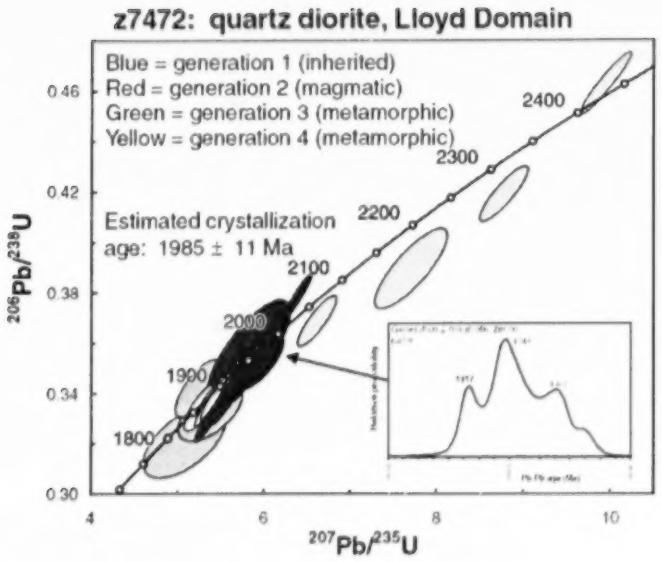

Figure 6.

SHRIMP U-Pb zircon results for z7472, quartz diorite, eastern Lloyd Domain. Inset shows a cumulative probability curve for generation 2 magmatic zircon.

although the prominence of the 1948 Ma mode makes it conceivable that this could instead represent the crystallization age, with the older dates being affected by inheritance.

Generation 3 zircon is characterized by low U (11–32 ppm) and Th/U of 0.1–0.5. The analytical uncertainties are relatively large owing to the low U, but the U-Pb results (n = 6) are within 5% of concordia and have $^{207}Pb/^{206}Pb$ dates of 1967 Ma to 1820 Ma. Excluding the youngest analysis, the weighted mean of five spots is 1941 ± 24 Ma (MSWD = 1.4; P = 24%), which is taken as an age of high-grade metamorphism recorded in the eastern Lloyd Domain.

Generation 4 fragments have U contents of 30–100 ppm and Th/U of about 0.2. Five concordant analyses have $^{207}Pb/^{206}Pb$ dates of 1902 Ma to 1876 Ma, with a weighted mean of 1897 ± 8 Ma (MSWD = 0.56; P = 69%). This result indicates that a second metamorphic event affected the rock.

z7473 (leucogranite, eastern Lloyd Domain)

Two morphological types of zircon are recognized from this sample (Fig. 7).

A) The first type is large (100–150 µm wide; l:w = 2–3:1), pale pink-brown prisms, with rounded grain edges, prominent fracturing, and minor clear inclusions. Some obvious structural cores are visible in reflected light. Backscattered electron images reveal bright, unzoned, or faintly banded to finely oscillatory-zoned zircon. A few structural cores are present that are bright in BSE images, but most are strongly altered and dull in BSE images. Most grains have an unzoned outer rim that is slightly darker in BSE images.

B) The second type is equant to stubby prismatic grains, 75–150 µm diameter, some with multifaceting, and others subrounded. Backscattered electron images are unzoned or show faint banded or weak sector zoning

Three generations of zircon growth are recognized. Generation 1 zircon comprises inherited zircon, and appears to be very minor. Magmatic zircon of generation 2 comprises most of the zircon making up both morphological types A and B. Examples of generation 2 growth in type A zircon can be seen in Figure 7b and 7c as the dominant areas of bright zircon, and in type B zircon in Figure 7d (grains 34, 36), where it appears as broadly and diffusely zoned. Structural cores such as shown in Figure 7b (grain 46) are also of generation 2 age. Zircon of generation 3 is present mainly in type A grains as thin rims, as clearly evident in Figure 7b and 7c, and is thought to be of metamorphic origin.

A total of 35 analyses were acquired from 29 grains (Fig. 8). None of the obvious structural cores, such as the one shown in Figure 7b (grain 46) proved to have dates indicative of inheritance; however, a single analysis of the central part of a type B rounded zircon (7473-15.1; Table 1) is 9% discordant and has a $^{207}Pb/^{206}Pb$ date of 2049 Ma. (Fig. 8). Despite the absence of obvious internal structures in this grain, the date is interpreted as being influenced by inheritance, with likely mixing with magmatic zircon of generation 2.

Thirty-three analyses of generation 2 zircon from type A and B zircons are all nearly concordant (Fig. 8), with U from 250–750 ppm and Th/U varying from 0.1–0.7. The $^{207}Pb/^{206}Pb$ dates range from 1997 Ma to 1901 Ma. The distribution of data on a relative probability curve (inset, Fig. 8) are negatively skewed, with a major peak at ca. 1972 Ma, consistent with variable extents of Pb-loss from a single original age. The weighted mean of the 18 oldest analyses is 1975 ± 5 (MSWD = 1.4; P = 14%), which is considered the crystallization age.

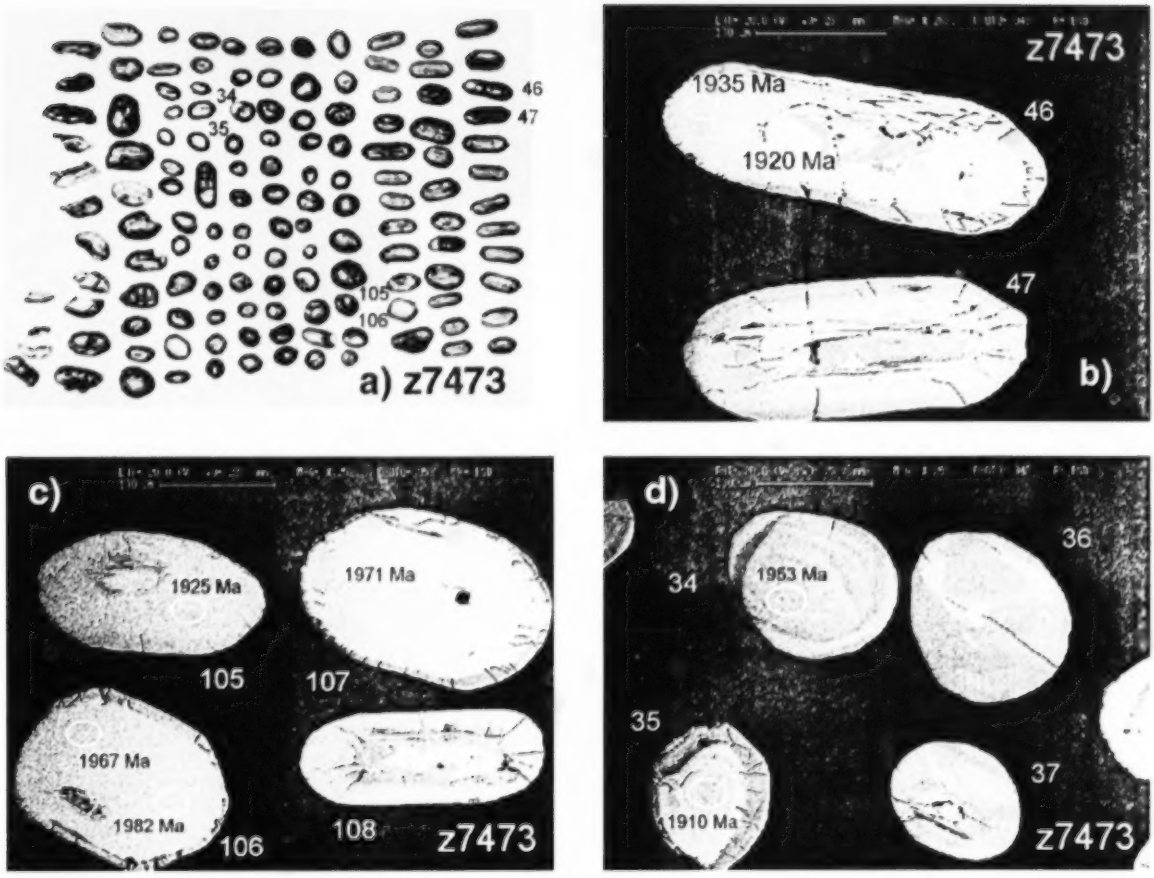

Figure 7. *Zircons from z7473, leucogranite, eastern Lloyd Domain;* ***a)*** *transmitted light,* ***b)–d)*** *backscattered electrons. Ellipses show locations of SHRIMP analysis sites and* $^{207}Pb/^{206}Pb$ *dates.*

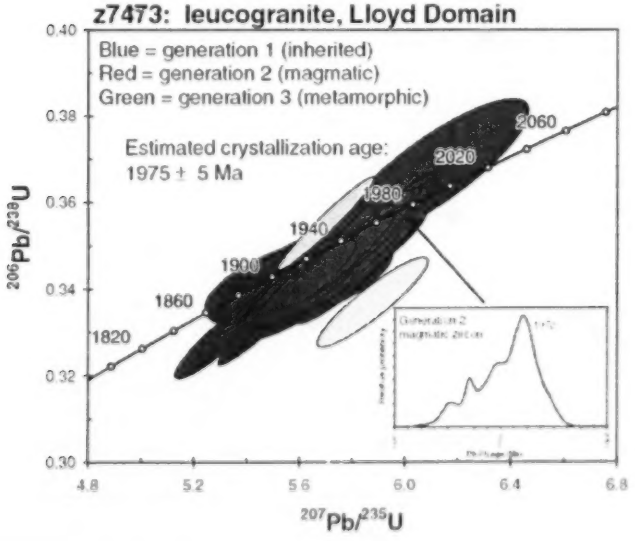

Figure 8.

SHRIMP U-Pb zircon results for z7473, leucogranite, eastern Lloyd Domain. Inset shows a cumulative probability curve for generation 2 magmatic zircon.

A single analysis of a thick rim of generation 3 zircon (7473-45.2; Table 1) was concordant at 1927 ± 34 Ma. The Th/U ratio of 0.5 is not distinguishable from the dominant generation 2 zircon. The core of this grain is made up of slightly discordant (5%) generation 2 zircon with a $^{207}Pb/^{206}Pb$ date of 1993 ± 16 Ma (7473-45.1; Table 1).

z7471 (granite, Clearwater Domain)

The zircons from this sample comprise two morphological types in roughly equal proportions (Fig. 9a).

A) The first type is prismatic grains (3–2:1; typically 50 µm wide), ranging from clear to moderately turbid, and possessing strong visible oscillatory zoning. The grain edges have slightly rounded face edges. The BSE images are bright and reveal fine oscillatory zoning, with recrystallization patches in some grains having overprinted the zoning, and variable secondary alteration. Structural cores are minor.

B) The second type is large, anhedral to subhedral, generally clear grain fragments and subrounded, whole, stubby prismatic grains. The BSE images are generally dark in comparison with type A, with broad-banded, sector, or nebulous zoning. Some grains are overgrown by thin rims of oscillatory zircon having bright BSE response.

Three generations of zircon growth are recognized from the images and SHRIMP analysis. Generation 1 comprises inherited zircon found as the dark BSE regions of type B and structural cores of type A. An example of such zircon is shown in grain 47 (Fig. 9c). Generation 2 is the oscillatory zircon found in both types A and B and is considered to be of magmatic origin. Examples are shown in Figures 9b and 9d. Generation 3 zircon comprises the recrystallization patches found in type A zircon, and likely of metamorphic or metasomatic origin. An example of a dated patch is shown in grain 45 (Fig. 9b).

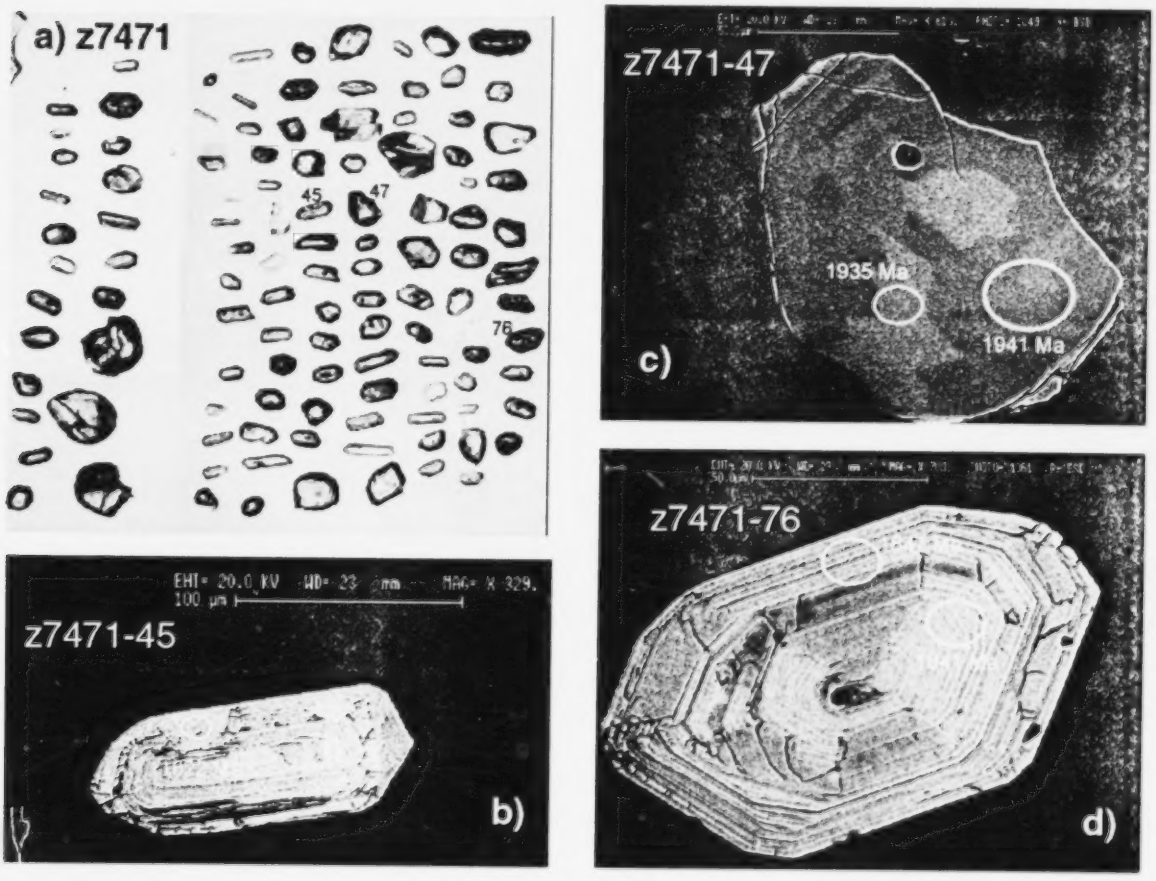

*Figure 9. Zircons from z7471, granite, Clearwater Domain; **a)** transmitted light, **b)–d)** backscattered electrons. Ellipses show locations of SHRIMP analysis sites and $^{207}Pb/^{206}Pb$ dates.*

A single analysis of a thick rim of generation 3 zircon (7473-45.2; Table 1) was concordant at 1927 ± 34 Ma. The Th/U ratio of 0.5 is not distinguishable from the dominant generation 2 zircon. The core of this grain is made up of slightly discordant (5%) generation 2 zircon with a $^{207}Pb/^{206}Pb$ date of 1993 ± 16 Ma (7473-45.1; Table 1).

z7471 (granite, Clearwater Domain)

The zircons from this sample comprise two morphological types in roughly equal proportions (Fig. 9a).

A) The first type is prismatic grains (3–2:1; typically 50 µm wide), ranging from clear to moderately turbid, and possessing strong visible oscillatory zoning. The grain edges have slightly rounded face edges. The BSE images are bright and reveal fine oscillatory zoning, with recrystallization patches in some grains having overprinted the zoning, and variable secondary alteration. Structural cores are minor.

B) The second type is large, anhedral to subhedral, generally clear grain fragments and subrounded, whole, stubby prismatic grains. The BSE images are generally dark in comparison with type A, with broad-banded, sector, or nebulous zoning. Some grains are overgrown by thin rims of oscillatory zircon having bright BSE response.

Three generations of zircon growth are recognized from the images and SHRIMP analysis. Generation 1 comprises inherited zircon found as the dark BSE regions of type B and structural cores of type A. An example of such zircon is shown in grain 47 (Fig. 9c). Generation 2 is the oscillatory zircon found in both types A and B and is considered to be of magmatic origin. Examples are shown in Figures 9b and 9d. Generation 3 zircon comprises the recrystallization patches found in type A zircon, and likely of metamorphic or metasomatic origin. An example of a dated patch is shown in grain 45 (Fig. 9b).

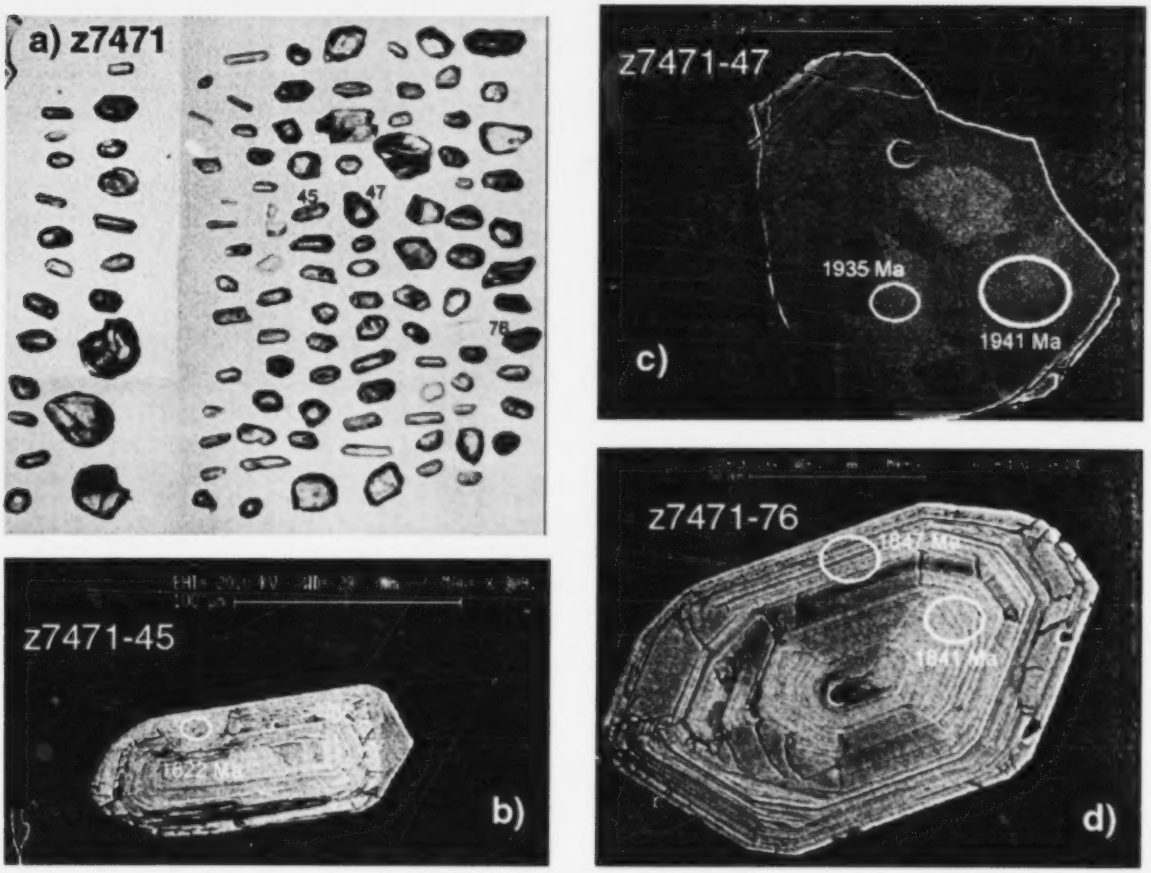

Figure 9. *Zircons from z7471, granite, Clearwater Domain;* ***a)*** *transmitted light,* ***b)–d)*** *backscattered electrons. Ellipses show locations of SHRIMP analysis sites and* $^{207}Pb/^{206}Pb$ *dates.*

A total of 24 spot dates were obtained from 16 grains (Fig. 10). The analyses of generation 1 inherited zircon are within 7% of concordia, and the $^{207}Pb/^{206}Pb$ dates are dominantly in the range 1900–1850 Ma. The weighted mean of eight analyses from six grains is 1873 ± 13 Ma (MSWD = 1.6; P = 12%). One grain (47.1, 47.2, Table 1) has a date of ca. 1940 Ma (Fig. 9c), and two spots on grain 28 gave a mean age of ca. 2545 Ma. These ages are interpreted to be inherited from the source region of the granite.

Analyses of generation 2 zircon are concordant within error and have $^{207}Pb/^{206}Pb$ dates from 1851 Ma to 1829 Ma. The weighted mean of all 11 spots analyzed is 1843 ± 4 Ma (MSWD = 0.63; P = 79%), which is taken as the crystallization age of the granite. Uranium concentrations range mostly from 500–800 ppm, with Th/U ratios of 0.2 to 0.4.

A single analysis of a generation 3 recrystallization patch on grain 45 (Fig. 9b, 10) yielded an age of 1822 ± 12 Ma. The Th/U value of 0.04 for this zircon is consistent with this result dating a fluid-related event.

z7475 (granitic gneiss xenolith within Clearwater Domain)

The zircons in this sample fall into two morphological varieties (Fig. 11):

A) The first type is prisms (~75 μm wide, aspect ratios 2–3:1), that are clear, colourless, fractured, and have rounded grain edges. The BSE images reveal relatively bright, diffuse oscillatory-zoned cores, with dark unzoned rims ranging from 5–100 μm wide.

B) Irregular to subequant grains, about 100–200 μm in diameter, are clear, colourless, and moderately fractured. In BSE images they range from dark and unzoned to weakly banded and may have cores with bright BSE response.

Two generations of growth are recognized from the imaging and dating. Generation 1 zircon represents the dominant magmatic growth, and is present as the oscillatory-zoned zircon of type A. Examples of generation 1 zircon occurring within type A morphology are shown in Figure 11b and 11c. Generation 2 zircon is considered to be of metamorphic origin, and forms the rims of type A zircon and most of the volume of type B grains. Generation 2 zircon is evident in the type B morphology (Fig. 11d).

A total of 21 spot U-Pb analyses were obtained from 16 grains (Fig. 12). Generation 1 is defined by 15 analyses of the interior portions of grains from zircon type A, characterized by U concentrations of 70–200 ppm and Th/U ratios from 0.6–1.4. Most data are concordant within error and have $^{207}Pb/^{206}Pb$ dates ranging from 2536 Ma to 1924 Ma (Fig. 12). These analyses spread well beyond analytical uncertainties, indicating that these grains are representative of more than one population. The cumulative probability curve for generation 1 zircon reveals a dominant mode at about 2483 Ma (Fig. 12). Multiple analyses of generation 1 zircon in grains 3 and 94 reveal large internal isotopic heterogeneities, whereby younger dates (1924 Ma and 2084 Ma, respectively) are measured from regions of generation 1 zircon that show diffuse or nonexistent zoning and which are darker in their BSE response. Analyses from regions of brighter BSE response adjacent outer regions retain older ages (i.e. 2482 Ma and 2525 Ma, respectively). Clearly the U-Pb system in the oscillatory-zoned cores has been partially disturbed. If we assume that a single age exists for generation 1 zircon that has been affected by younger events, a possible crystallization age of 2529 ± 16 Ma

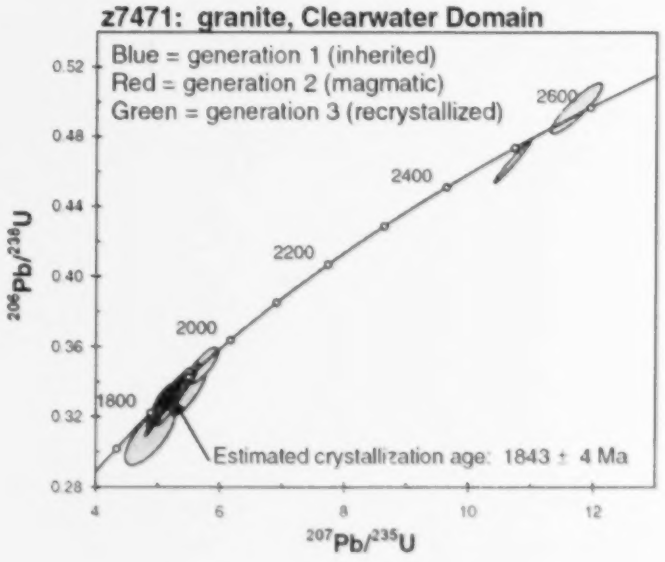

Figure 10.

SHRIMP U-Pb zircon results for z7471, granite, Clearwater Domain.

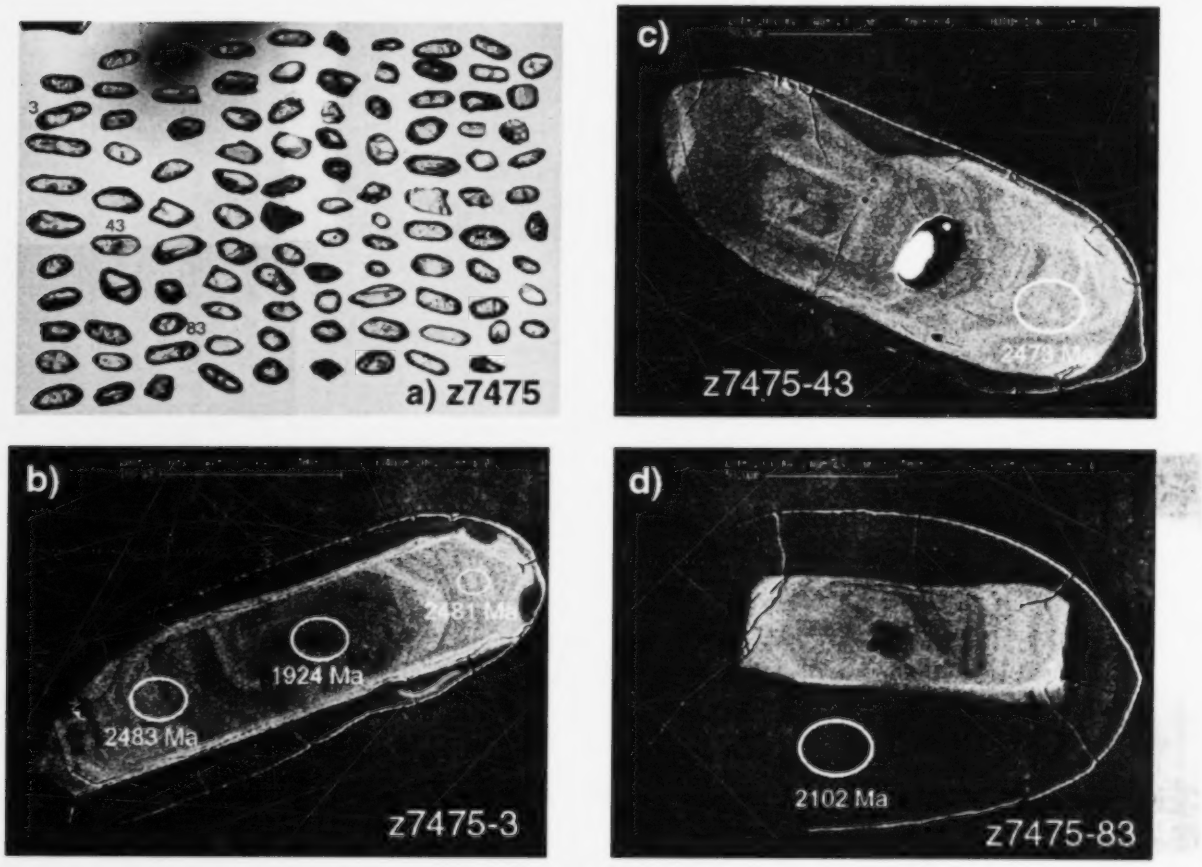

Figure 11. *Zircons from z7475, granitoid gneiss inclusion, Clearwater Domain;* ***a)*** *transmitted light,* ***b)–d)*** *backscattered electrons. Ellipses show locations of SHRIMP analysis sites and $^{207}Pb/^{206}Pb$ dates.*

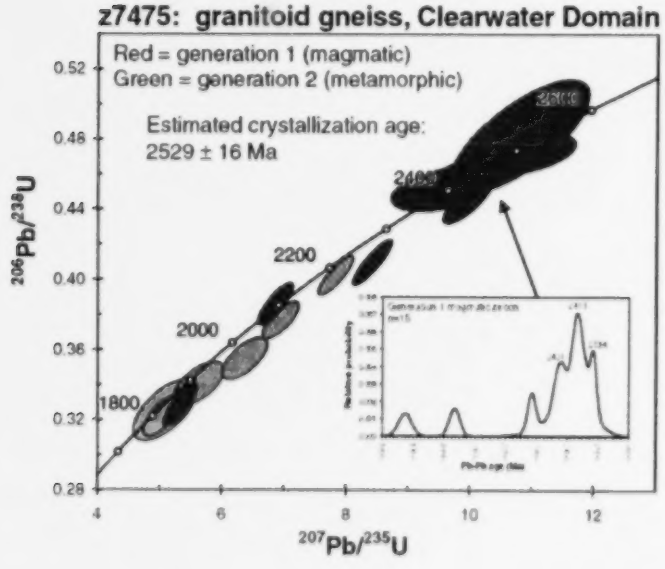

Figure 12.

SHRIMP U-Pb zircon results for z7475, granitoid gneiss inclusion, Clearwater Domain. Inset shows a cumulative probability curve for generation 1 magmatic zircon.

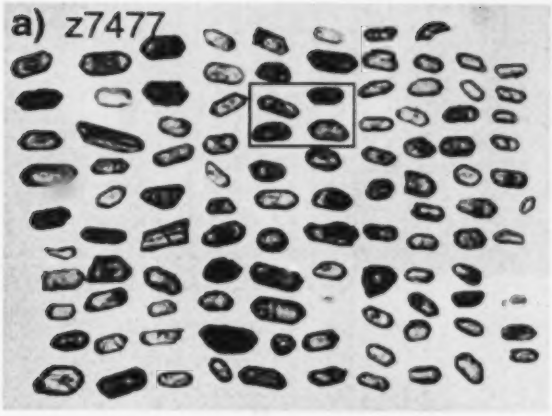

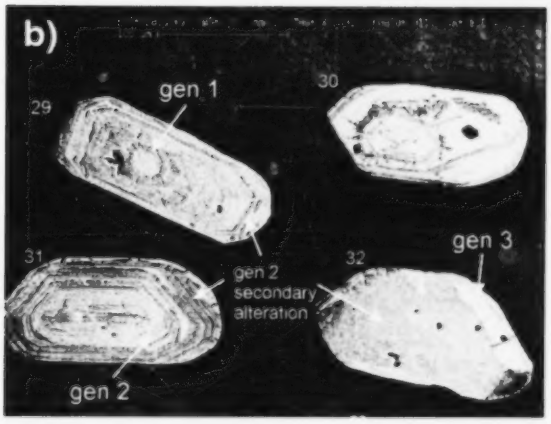

Figure 13. *Zircons from z7477, 'Wylie-type' granodiorite from the western Lloyd Domain;* ***a)*** *transmitted light,* ***b)–d)*** *backscattered electrons; gen = generation. Ellipses show locations of SHRIMP analysis sites and* $^{207}Pb/^{206}Pb$ *dates.*

(MSWD = 0.61, P = 61%) is calculated based on the weighted mean of the four oldest analyses. It is also conceivable that the crystallization age is closer to 2485 Ma, the main peak on the probably curve, but it is difficult to distinguish these possibilities with the current data set. In any event, the protolith appears to be ca. 2.5 Ga.

Six analyses of generation 2 unzoned rims and fragments have U concentrations between 11 ppm and 40 ppm, Th/U = 0.4–0.9, and $^{207}Pb/^{206}Pb$ dates from 2242 Ma to 1855 Ma. One analysis each from grains 63 and 27 together indicate an age of 1856 ± 56 Ma. The older analyses of generation 2 zircon are slightly discordant, and are consistent with lying along a mixing trend towards the older cores (Fig. 12). It appears that the overgrowths may have inherited their isotopic composition, in part, from the cores. Accordingly, the age of metamorphism is most probably recorded by the imprecise 1856 Ma result. It is noted that this age is within error of the estimated crystallization age of the host granite (z7471).

z7477 ('Wylie-type' granodiorite, western Lloyd Domain)

The zircons recovered from the core sample (Fig. 13) comprise exclusively prisms (some twinned grains) and prism fragments, 50–100 μm wide (aspect ratios of 2–4:1), colourless to turbid, with visible oscillatory zoning, and some obvious structural cores. In BSE images, the grains display typically well developed, fine oscillatory zoning, although in some interior zones the zoning is broader and more diffuse. Dark, secondary alteration zones parallel the primary zoning, and bright recrystallization patches present in some grains crosscut all features.

Three generations of zircon growth are recognized. Generation 1 zircon comprises small inherited cores that have nebulous and relatively dark zoning in BSE images and have an irregular boundary against generation 2 zircon (e.g. grain 29, Fig. 13b). Other structural cores having weakly

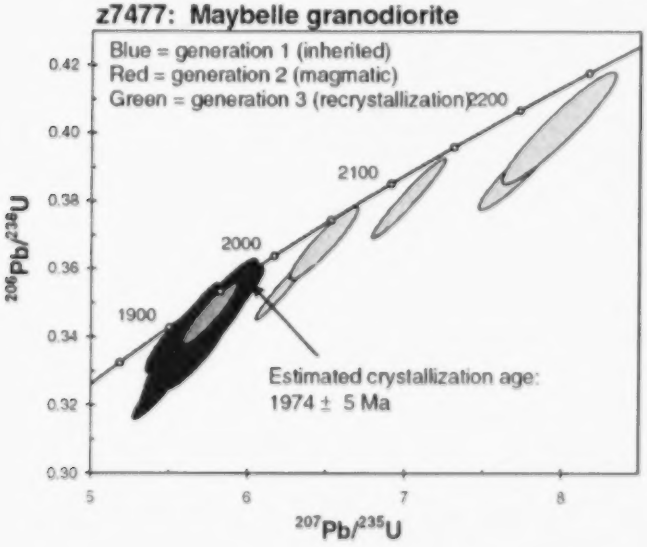

Figure 14.

SHRIMP U-Pb zircon results for z7477 'Wylie-type' granodiorite, western Lloyd Domain.

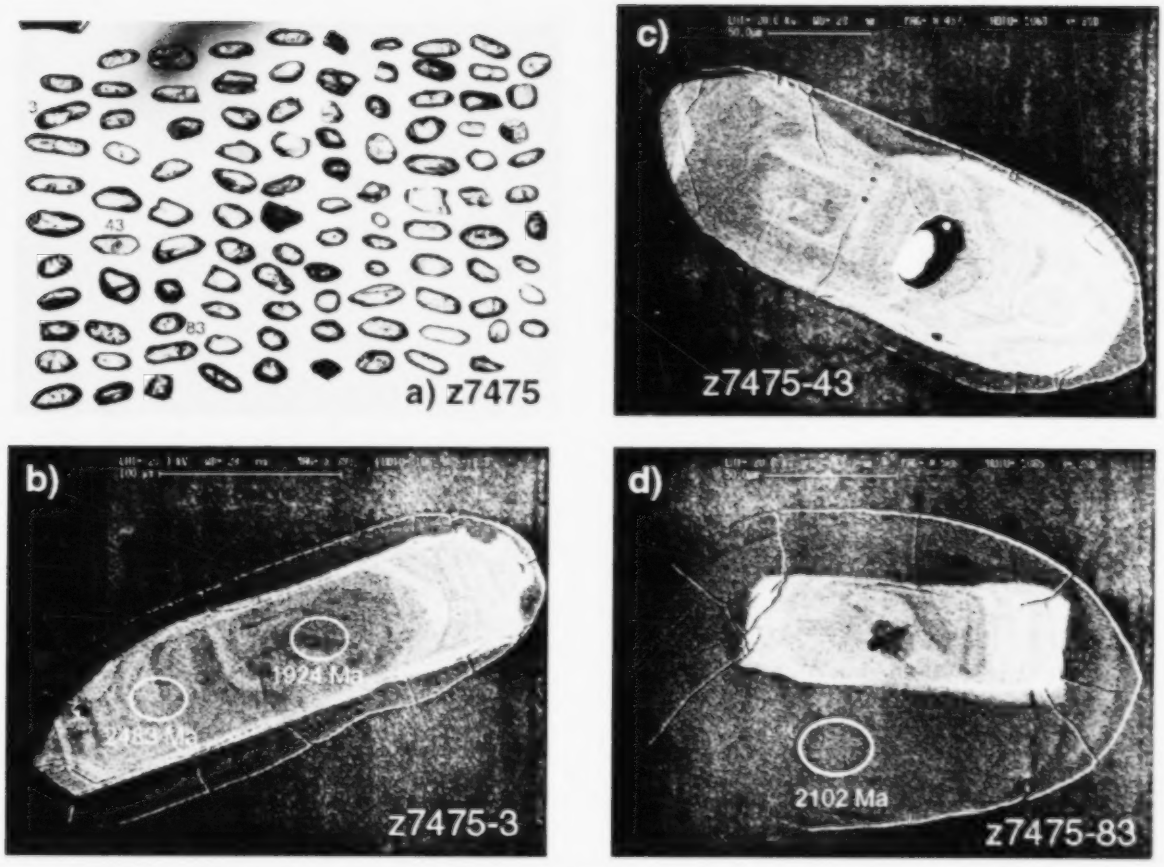

Figure 11. *Zircons from z7475, granitoid gneiss inclusion, Clearwater Domain: **a)** transmitted light, **b)–d)** backscattered electrons. Ellipses show locations of SHRIMP analysis sites and $^{207}Pb/^{206}Pb$ dates.*

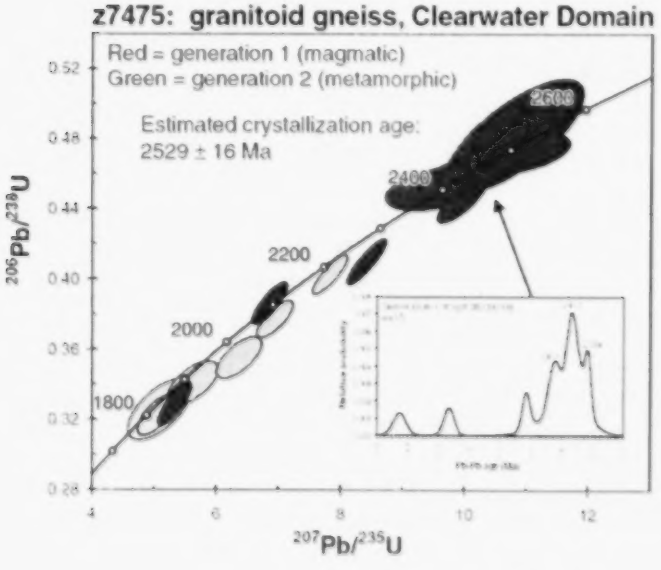

Figure 12.

SHRIMP U-Pb zircon results for z7475, granitoid gneiss inclusion, Clearwater Domain. Inset shows a cumulative probability curve for generation 1 magmatic zircon.

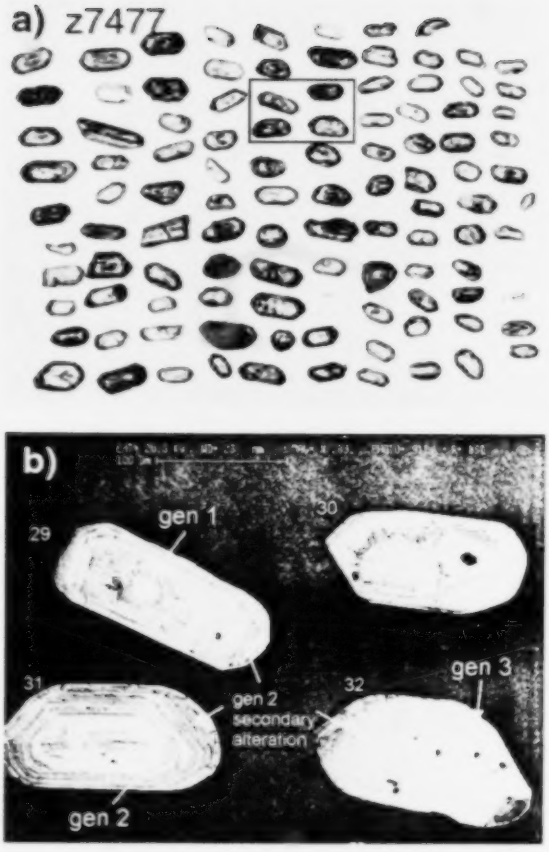

*Figure 13. Zircons from z7477, 'Wylie-type' granodiorite from the western Lloyd Domain; **a)** transmitted light, **b)–d)** backscattered electrons; gen = generation. Ellipses show locations of SHRIMP analysis sites and $^{207}Pb/^{206}Pb$ dates.*

(MSWD = 0.61, P = 61%) is calculated based on the weighted mean of the four oldest analyses. It is also conceivable that the crystallization age is closer to 2485 Ma, the main peak on the probably curve, but it is difficult to distinguish these possibilities with the current data set. In any event, the protolith appears to be ca. 2.5 Ga.

Six analyses of generation 2 unzoned rims and fragments have U concentrations between 11 ppm and 40 ppm, Th/U = 0.4–0.9, and $^{207}Pb/^{206}Pb$ dates from 2242 Ma to 1855 Ma. One analysis each from grains 63 and 27 together indicate an age of 1856 ± 56 Ma. The older analyses of generation 2 zircon are slightly discordant, and are consistent with lying along a mixing trend towards the older cores (Fig. 12). It appears that the overgrowths may have inherited their isotopic composition, in part, from the cores. Accordingly, the age of metamorphism is most probably recorded by the imprecise 1856 Ma result. It is noted that this age is within error of the estimated crystallization age of the host granite (z7471).

z7477 ('Wylie-type' granodiorite, western Lloyd Domain)

The zircons recovered from the core sample (Fig. 13) comprise exclusively prisms (some twinned grains) and prism fragments, 50–100 µm wide (aspect ratios of 2–4:1), colourless to turbid, with visible oscillatory zoning, and some obvious structural cores. In BSE images, the grains display typically well developed, fine oscillatory zoning, although in some interior zones the zoning is broader and more diffuse. Dark, secondary alteration zones parallel the primary zoning, and bright recrystallization patches present in some grains crosscut all features.

Three generations of zircon growth are recognized. Generation 1 zircon comprises small inherited cores that have nebulous and relatively dark zoning in BSE images and have an irregular boundary against generation 2 zircon (e.g. grain 29, Fig. 13b). Other structural cores having weakly

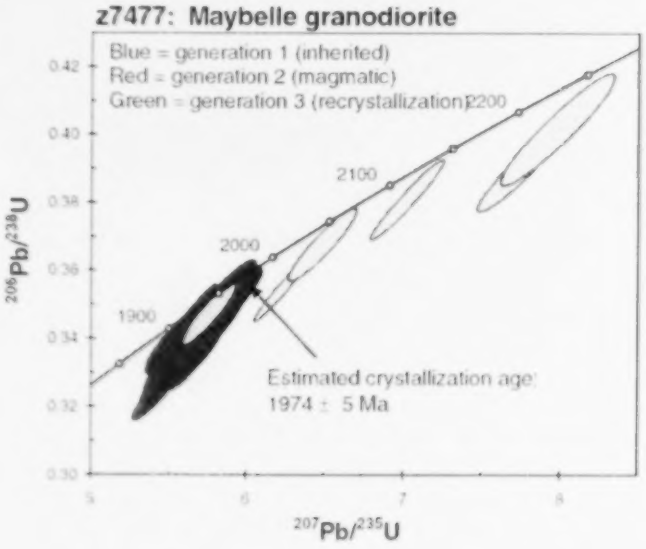

Figure 14.

SHRIMP U-Pb zircon results for z7477 'Wylie-type' granodiorite, western Lloyd Domain.

banded zircon have a regular outer boundary, and based upon age results (below) are apparently early components of generation 2 growth (e.g. grain 30, Fig. 13b). Typical generation 2 magmatic zircon is characterized by prominent oscillatory zoning, except where pervasively overprinted by secondary alteration (e.g. grain 31, Fig. 13b). Generation 3 comprises recrystallization patches having bright BSE response (grain 32, Fig. 13b).

A total of 23 SHRIMP analyses were obtained from 15 grains (Fig. 14). Analyses of generation 1 inherited cores (five analyses from five grains) yielded dates ranging from 2276 Ma to 2060 Ma, all slightly discordant. Uranium concentrations varied widely, from 250–4000 ppm, with Th/U about 0.4.

Seventeen analyses of generation 2 zircon have $^{207}Pb/^{206}Pb$ dates ranging from 1997 Ma to 1925 Ma and are 1–8% discordant (Table 1; Fig. 14). Uranium abundances are 150–3600 ppm and Th/U = 0.2–2.3. Excluding the two youngest analyses as possibly having suffered Pb loss yields a weighted mean (n = 15) of 1974 ± 5 Ma (MSWD = 1.6; P = 8%), taken as the crystallization age of the granodiorite.

A single analysis of a recrystallization patch (grain 59) yielded a date of 1959 ± 18 Ma. This result is within error of the crystallization age, and suggests that recrystallization was related to postmagmatic hydrothermal alteration.

z7478 (Fishing Creek quartz diorite, Taltson magmatic zone)

The zircons recovered from this sample comprise two morphological types (Fig. 15).

A) The first type is stubby to elongate prisms (aspect ratios 2–5:1), clear to turbid, colourless to brown, oscillatory zoned, 50–100 µm wide, with visible cores in some. In BSE images, the grains are bright to variably dark in altered regions, commonly oscillatory zoned, with bright crosscutting recrystallized patches.

B) The second type is in minor abundance, equant to slightly elongate, colourless to turbid, moderately fractured, 80–150 µm in diameter. In BSE images, dark, featureless to weakly zoned.

Three generations of zircon growth are recognized, identical to those described for z7477. A possible inherited generation 1 core is shown in grain 81 (Fig. 15c). Figure 15b shows several grains comprised almost entirely of generation 2 magmatic zircon. A generation 3 crosscutting recrystallization patch is shown in grain 82 (Fig. 15c).

A total of 27 analyses were obtained from 22 grains (Fig. 16). Generation 1 inherited cores have U contents of 160–340 ppm and Th/U=0.1–0.7. Four analyses from four grains have $^{207}Pb/^{206}Pb$ dates of 2316–2002 Ma and 1937 Ma and all are about 5% discordant. The youngest core analysis is from grain 63 and is younger than the magmatic overgrowth.

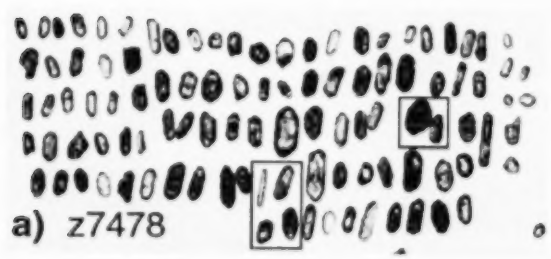

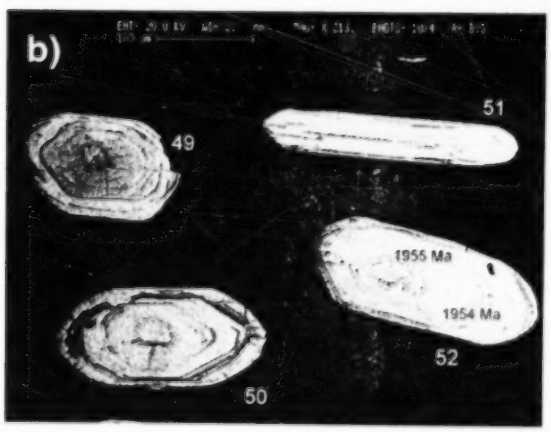

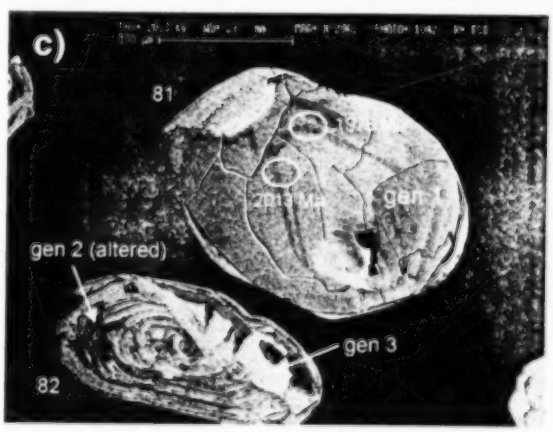

Figure 15. *Zircons from z7478, Fishing Creek quartz diorite, Taltson magmatic zone; **a**) transmitted light, **b**)–**d**) backscattered electrons; gen = generation. Ellipses show locations of SHRIMP analysis sites and $^{207}Pb/^{206}Pb$ dates.*

banded zircon have a regular outer boundary, and based upon age results (below) are apparently early components of generation 2 growth (e.g. grain 30, Fig. 13b). Typical generation 2 magmatic zircon is characterized by prominent oscillatory zoning, except where pervasively overprinted by secondary alteration (e.g. grain 31, Fig. 13b). Generation 3 comprises recrystallization patches having bright BSE response (grain 32, Fig. 13b).

A total of 23 SHRIMP analyses were obtained from 15 grains (Fig. 14). Analyses of generation 1 inherited cores (five analyses from five grains) yielded dates ranging from 2276 Ma to 2060 Ma, all slightly discordant. Uranium concentrations varied widely, from 250–4000 ppm, with Th/U about 0.4.

Seventeen analyses of generation 2 zircon have $^{207}Pb/^{206}Pb$ dates ranging from 1997 Ma to 1925 Ma and are 1–8% discordant (Table 1; Fig. 14). Uranium abundances are 150–3600 ppm and Th/U = 0.2–2.3. Excluding the two youngest analyses as possibly having suffered Pb loss yields a weighted mean (n = 15) of 1974 ± 5 Ma (MSWD = 1.6; P = 8%), taken as the crystallization age of the granodiorite.

A single analysis of a recrystallization patch (grain 59) yielded a date of 1959 ± 18 Ma. This result is within error of the crystallization age, and suggests that recrystallization was related to postmagmatic hydrothermal alteration.

z7478 (Fishing Creek quartz diorite, Taltson magmatic zone)

The zircons recovered from this sample comprise two morphological types (Fig. 15).

A) The first type is stubby to elongate prisms (aspect ratios 2–5:1), clear to turbid, colourless to brown, oscillatory zoned, 50–100 µm wide, with visible cores in some. In BSE images, the grains are bright to variably dark in altered regions, commonly oscillatory zoned, with bright crosscutting recrystallized patches.

B) The second type is in minor abundance, equant to slightly elongate, colourless to turbid, moderately fractured, 80–150 µm in diameter. In BSE images, dark, featureless to weakly zoned.

Three generations of zircon growth are recognized, identical to those described for z7477. A possible inherited generation 1 core is shown in grain 81 (Fig. 15c). Figure 15b shows several grains comprised almost entirely of generation 2 magmatic zircon. A generation 3 crosscutting recrystallization patch is shown in grain 82 (Fig. 15c).

A total of 27 analyses were obtained from 22 grains (Fig. 16). Generation 1 inherited cores have U contents of 160–340 ppm and Th/U=0.1–0.7. Four analyses from four grains have $^{207}Pb/^{206}Pb$ dates of 2316–2002 Ma and 1937 Ma and all are about 5% discordant. The youngest core analysis is from grain 63 and is younger than the magmatic overgrowth,

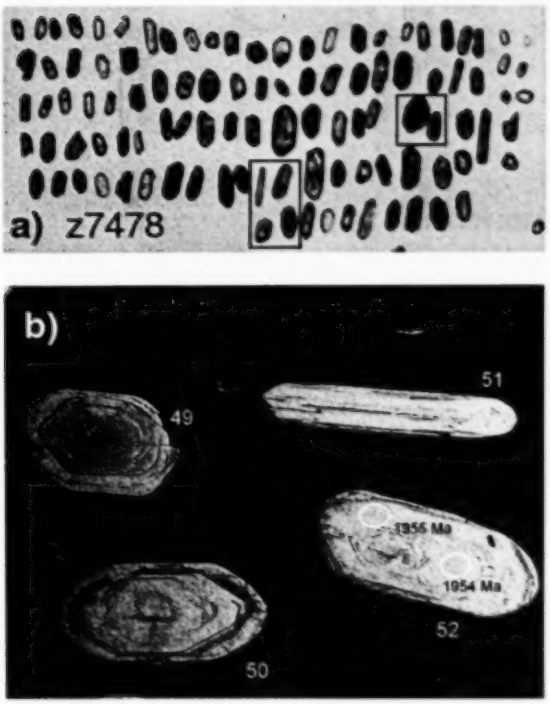

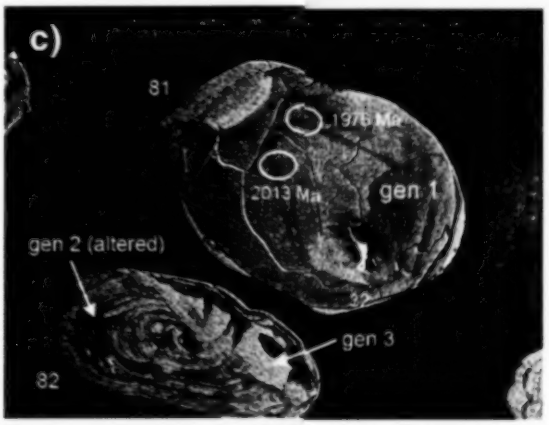

Figure 15. *Zircons from z7478, Fishing Creek quartz diorite, Taltson magmatic zone;* ***a)*** *transmitted light,* ***b)–d)*** *backscattered electrons; gen = generation. Ellipses show locations of SHRIMP analysis sites and $^{207}Pb/^{206}Pb$ dates.*

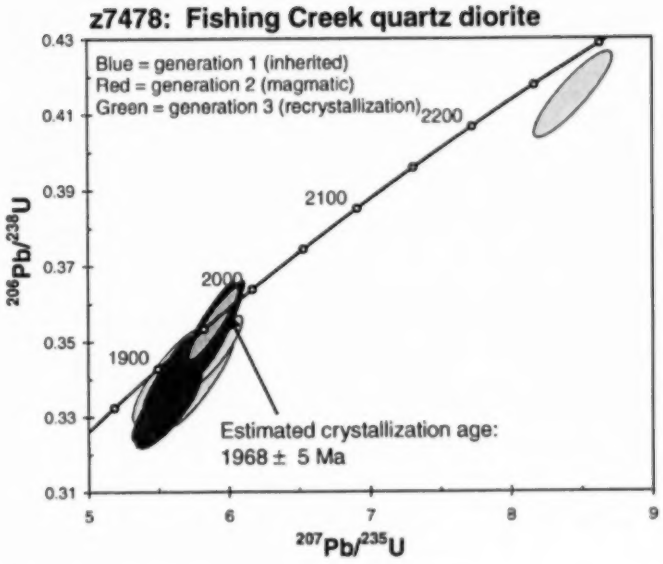

Figure 16.

SHRIMP U-Pb zircon results for z7478, Fishing Creek quartz diorite, Taltson magmatic zone.

indicating that it has lost Pb. The disturbance of the inherited core ages is illustrated in Figure 15c in which two spots on grain 81 yielded ages of 2013 Ma and 1976 Ma.

Analyses (n = 22) of generation 2 magmatic zircon have U of 90–900 ppm and Th/U = 0.1–0.7. The $^{207}Pb/^{206}Pb$ dates range from 1985 Ma and 1923 Ma and are less than 5% discordant (Fig. 16). These data do not form a single age population within analytical errors, however, if the youngest four analyses are excluded, the weighted mean of 1968 ± 5 Ma (MSWD = 1.4, P = 11%) is just statistically coherent. It is noted that the two youngest analyses rejected have anomalously low Th/U. The 1968 Ma result is considered a reasonable estimate of the crystallization of the quartz diorite.

A single analysis of a generation 3 recrystallized patch on grain 80 yielded a date of 1959 ±16 Ma, identical to the result for z7477. This zircon has low Th/U (0.08), and possibly resulted from late magmatic hydrothermal recrystallization.

SUMMARY

Table 2 presents a summary of the SHRIMP U-Pb zircon results for the seven granitoid samples from the southern and southwestern margins of the Athabasca Basin. The salient features of the geochronology are listed below.

1) Granite from the Virgin River shear zone is imprecisely dated at ca. 1.83 Ga.

2) The eastern Lloyd Domain is underlain by granitoid rocks that are ca. 1.98 Ga. These rocks were either sourced within, or intruded, crust of ca. 2.4–2.0 Ga age. The 1.98 Ga ages are characteristic of the Taltson magmatic zone.

3) The Clearwater Domain comprises 1.843 Ga granite with inclusions of 2.53 Ga granitic gneiss. The latter may be representative of the age of source rocks to the granite.

4) Granodioritic basement rocks within the western Lloyd Domain and within the southerly extensions of the Taltson magmatic zone crystallized at ca. 1.97 Ga.

ACKNOWLEDGMENTS

The results stem from Geochronology Project P297. The manuscript was reviewed by Vicki McNicoll.

REFERENCES

Annesley, I.R., Madore, C., Krogh, T.E., Kwok, Y.Y., and Kamo, S.L.
1999: New U-Pb zircon and monazite geochronological results for Archean and Paleoproterozoic basement to the southeastern part of the Athabasca Basin, Saskatchewan; *in* Summary of Investigations 1999; Saskatchewan Geological Survey, Saskatchewan Energy and Mines, Miscellaneous Report 99-4.2, p. 90–99.

Bickford, M.E., Collerson, K.D., and Lewry, J.F.
1994: Crustal history of the Rae and Hearne provinces, southwestern Canadian Shield, Saskatchewan: constraints from geochronologic and isotopic data; Precambrian Research, v. 68, p. 1–21.

Card, C.
2001: Basement rocks to the western Athabasca Basin in Saskatchewan; *in* Summary of Investigations 2001; Saskatchewan Geological Survey, Saskatchewan Energy and Mines, Miscellaneous Report 2001-4-2, p. 321–333.

Cumming, G.L. and Richards, J.R.
1975: Ore lead isotope ratios in a continuously changing earth; Earth and Planetary Science Letters, v. 28, p. 155–171.

Jaffey, A.H., Flynn, K.F., Glendenin, L.E., Bentley, W.C., and Essling, A.M.
1971: Precision measurement of half-lives and specific activities of ^{235}U and ^{238}U; Physical Review C, v. 4, p. 1889–1906.

Jefferson, C.W., Delaney, G., and Olson, R.A.
2002: EXTECH IV Athabasca uranium multidisciplinary study: mid-year 2002-03 overview and impact analysis; *in* Summary of Investigations 2002; Saskatchewan Geological Survey, Saskatchewan Industry and Resources, Miscellaneous Report 2002-4.2, CD-ROM, Paper D-1, 12 p.

Lewry, J.F. and Sibbald, T.I.I.
1977: Variation in lithology and tectonometamorphic relationships in the Precambrian basement of northern Saskatchewan; Canadian Journal of Earth Sciences, v. 14, p. 1453–1467.

Ludwig, K.R.
2001: User's manual for Isoplot/Ex rev. 2.49: a Geochronological Toolkit for Microsoft Excel; Berkeley Geochronology Center, Special Publication 1a, 55 p.

McDonough, M.R., McNicoll, V.J., Schetselaar, E.M., and Grover, T.W.
2000: Geochronological and kinematic constraints on crustal shortening and escape in a wo-sided oblique-slip collisional and magmatic orogen, Paleoproterozoic Taltson magmatic zone, northeastern Alberta; Canadian Journal of Earth Sciences, v. 37, p. 1549–1573.

McNicoll, V.J., Thériault, R.J., and McDonough, M.R.
2000: Taltson basement gneissic rocks: U-Pb and Nd isotopic constraints on the basement to the Paleoproterozoic Taltson magmatic zone, northeastern Alberta; Canadian Journal of Earth Sciences, v. 37, p. 1575–1596.

Ross, G.M., Parrish, R.R., Villeneuve, M.E., and Bowring, S.A.
1991: Geophysics and geochronology of the crystalline basement of the Alberta Basin, western Canada; Canadian Journal of Earth Sciences, v. 28, p. 512–522.

Sibbald, T.I.I.
1974: La Loche (north) area: Reconnaissance geological survey of 74-C-NW and 74-C-NE; *in* Summary of Field Investigations by the Saskatchewan Geological Survey; Saskatchewan Department of Mines and Resources, p. 38–45.

Stern, R.A.
1996: A SHRIMP II ion microprobe at the Geological Survey of Canada; Geoscience Canada, v. 23, p. 73–76.
1997: The GSC Sensitive High Resolution Ion Microprobe (SHRIMP): analytical techniques of zircon U-Th-Pb age determinations and performance evaluation; *in* Current Research 1997-F, Geological Survey of Canada, p. 1–31.
2001: A new isotopic and trace element standard for the ion microprobe: preliminary TIMS U-Pb and electron microprobe data; Radiogenic Age and Isotopic Studies: Report 14; Geological Survey of Canada, Current Research 2001-F1, 11 p.

Stern, R.A. and Amelin, Y.
2003: Assessment of errors in SIMS zircon U-Pb geochronology using a natural zircon standard and NIST SRM 610 glass; Chemical Geology, v. 197, p. 111–146.

Williams, I.S.
1998: U-Th-Pb geochronology by ion microprobe; *in* Applications of Microanalytical Techniques to Understanding Mineralizing Processes, (ed.) M.A. McKibben, W.C.P. Shanks III, and W.I. Ridley; Reviews in Economic Geology, v. 7, Socorro, New Mexico, Society of Economic Geologists, p. 1–35.

Wilson, J.A.
1986: Geology of the basement beneath the Athabasca Basin in Alberta; Alberta Research Council, Bulletin 55, 61 p.